Smooth muscle cells of human veins show an increased response to injury at valve sites

Shinsuke Kikuchi, MD,[a] Lihua Chen, PhD,[b] Kevin Xiong, BS,[b] Yukihiro Saito, MD, PhD,[a] Nobuyoshi Azuma, MD,[a] Gale Tang, MD,[b,c,d] Michael Sobel, MD,[b,d] Thomas N. Wight, PhD,[c,e] *and* Richard D. Kenagy, PhD,[b,c] *Asahikawa, Japan; and Seattle, Wash*

ABSTRACT

Objective: Venous valves are essential but are prone to injury, thrombosis, and fibrosis. We compared the behavior and gene expression of smooth muscle cells (SMCs) in the valve sinus vs nonvalve sites to elucidate biologic differences associated with vein valves.

Methods: Tissue explants of fresh human saphenous veins were prepared, and the migration of SMCs from explants of valve sinus vs nonvalve sinus areas was measured. Proliferation and death of SMCs were determined by staining for Ki67 and terminal deoxynucleotidyl transferase dUTP nick end labeling. Proliferation and migration of passaged valve vs nonvalve SMCs were determined by cell counts and using microchemotaxis chambers. Global gene expression in valve vs nonvalve intima-media was determined by RNA sequencing.

Results: Valve SMCs demonstrated greater proliferation in tissue explants compared with nonvalve SMCs (19.3% ± 5.4% vs 6.8% ± 2.0% Ki67-positive nuclei at 4 days, respectively; mean ± standard error of the mean, five veins; $P < .05$). This was also true for migration (18.2 ± 2.7 vs 7.5 ± 3.0 migrated SMCs/explant at 6 days, respectively; 24 veins, 15 explants/vein; $P < .0001$). Cell death was not different (39.6% ± 16.1% vs 41.5% ± 16.0% terminal deoxynucleotidyl transferase dUTP nick end labeling-positive cells, respectively, at 4 days, five veins). Cultured valve SMCs also proliferated faster than nonvalve SMCs in response to platelet-derived growth factor subunit BB (2.9 ± 0.2-fold vs 2.1 ± 0.2-fold of control, respectively; $P < .001$; $n = 5$ pairs of cells). This was also true for migration (6.5 ± 1.2-fold vs 4.4 ± 0.8-fold of control, respectively; $P < .001$; $n = 7$ pairs of cells). Blockade of fibroblast growth factor 2 (FGF2) inhibited the increased responses of valve SMCs but had no effect on nonvalve SMCs. Exogenous FGF2 increased migration of valve but not of nonvalve SMCs. Unlike in the isolated, cultured cells, blockade of FGF2 in the tissue explants did not block migration of valve or nonvalve SMCs from the explants. Thirty-seven genes were differentially expressed by valve compared with nonvalve intimal-medial tissue (11 veins). Peptide-mediated inhibition of *SEMA3A*, one of the differentially expressed genes, increased the number of migrated SMCs of valve but not of nonvalve explants.

Conclusions: Valve compared with nonvalve SMCs have greater rates of migration and proliferation, which may in part explain the propensity for pathologic lesion formation in valves. Whereas FGF2 mediates these effects in cultured SMCs, the mediators of these stimulatory effects in the valve wall tissue remain unclear but may be among the differentially expressed genes discovered in this study. One of these genes, *SEMA3A*, mediates a valve-specific inhibitory effect on the injury response of valve SMCs. (J Vasc Surg 2018;67:1556-70.)

Clinical Relevance: Valves are a common site of venous thrombosis and of vein graft lesions. However, there is essentially nothing known about the response to injury of either animal or human valve sinus cells. The novel observation that the smooth muscle cells of the human valve sinus exhibit an exaggerated response to injury compared with smooth muscle cells of the nonvalve wall may help explain the propensity of the valves to fail after thrombotic events and for the valve wall to fail in arterial bypass grafts.

The venous valve is essential to normal circulatory function, with chronic venous disease marked by loss of valve function.[1] Valves are a common site of venous thrombosis,[2] which often leads to scarring, valve dysfunction, and post-thrombotic syndrome.[3] Finally, when saphenous veins are used for arterial bypass, stenotic lesions frequently occur at valve sites.[4-7]

Studies in mice have led to a good understanding of the role of endothelial cells in venous valve development.[8] There is also a reasonable understanding of the

From the Department of Vascular Surgery, Asahikawa Medical University, Asahikawa[a]; and the Department of Surgery,[b] Center for Cardiovascular Biology,[c] and Division of Vascular Surgery, VA Puget Sound Health Care System,[d] University of Washington, and the Matrix Biology Program, Benaroya Research Institute,[e] Seattle.

This work was supported by National Institutes of Health grant HL30946 (M.S. and R.D.K.), a VA Research and Development Merit Review Award (M.S.), and JSPS KAKENHI Grant 16K19962 (S.K.). For the RNA sequencing experiment, we are grateful for the generous support of the Matthew Endicott Fund (M.S. and R.D.K.).

Author conflict of interest: none.

Additional material for this article may be found online at www.jvascsurg.org.

Correspondence: Richard D. Kenagy, PhD, Research Assistant Professor, University of Washington, Center for Cardiovascular Biology and Department of Surgery, 850 Republican St, Brotman 333, Seattle, WA 98109 (e-mail: rkenagy@u.washington.edu).

The editors and reviewers of this article have no relevant financial relationships to disclose per the JVS policy that requires reviewers to decline review of any manuscript for which they may have a conflict of interest.

0741-5214

http://dx.doi.org/10.1016/j.jvs.2017.03.447

venous response to injury from studies of arterialized animal vein grafts and of human veins and venous tissue perfused or cultured ex vivo,[9-11] but there is essentially nothing known about the response to injury of the animal or human venous valve wall area specifically. Our approach has been to use human venous tissue explants as an ex vivo model of injury. We have previously shown that arterial tissue explants demonstrate many of the same responses observed in the injured artery in vivo. For example, growth factor requirements for cell migration as well as the kinetics of cell migration, proliferation, and production of matrix-degrading proteinases are the same in vivo as in tissue explants.[12-14]

Whereas the rheology and hemodynamics at the valve sinus may underlie some of the problems at valve sites, we hypothesized that there are unique biologic and cellular characteristics of the venous smooth muscle cell (SMC) at valve sites. Using human saphenous veins, we now report an exaggerated response to injury by SMCs of the valve wall as evidenced by increased SMC proliferation and migration compared with nonvalve wall SMCs.

ARTICLE HIGHLIGHTS

- **Type of Research:** Basic science investigation into activation and proliferation differences of vein valve site smooth muscle cells compared with nonvalve site smooth muscle cells
- **Take Home Message:** Valve site compared with nonvalve site smooth muscle cells had increased proliferation and migration but not cell death. This may be mediated in part by fibroblast growth factor.
- **Recommendation:** Further in vivo work will clarify mechanisms, but this is an important finding that may explain vein valve site stenoses in human bypasses.

METHODS

Methods are briefly outlined here. Complete methods are available online (Supplementary Methods, online only).

Veins, tissue culture, and cell culture. Human saphenous vein remnants were obtained from patients undergoing coronary artery bypass or peripheral vascular bypass operations. All subjects gave informed consent as approved by the Institutional Review Boards of the University of Washington and the Benaroya Research Institute (the latter for anonymous tissues only, which provided the majority of subjects). After dissection of periadventitial tissue and removal of the endothelium and valve leaflets, segments of valve sinus were separated from remaining segments (Supplementary Fig 1, online only). The intimal-medial layer containing SMCs was dissected from the adventitia, and uniform explants of both layers were made using a tissue chopper. Migration of cells from tissue explants was assessed daily, as follows: (1) an explant was called migration positive if at least one attached, spread cell was observed outside the explant; and (2) the number of migrated cells (up to 100) was counted for each explant. The first method measures only migration, whereas the second method measures the combination of migration and post-migration proliferation.[13-15] When needed, various reagents were added with the growth medium, which was changed every 2 days. Cells obtained from explants were passaged and used for subsequent experiments.

Tissue histology and immunostaining. To compare SMC proliferation (Ki67 immunostaining) and death (terminal deoxynucleotidyl transferase dUTP nick end labeling) in valve vs nonvalve wall, veins were cleaned of periadventitial tissue and opened longitudinally. Specimens with contiguous valve and nonvalve areas were cut into 2-mm-wide, full-thickness (ie, with adventitia and intima-media) longitudinal specimens and cultured up to 4 days.

Cell migration, growth, and attachment. Cell migration was performed using both microchemotaxis chambers (Neuro Probe, Inc, Gaithersburg, Md)[16] and scratch migration assays. A 3-day growth assay and the crystal violet assay were used to measure growth and attachment, respectively.[16]

RNA sequencing and pathway enrichment analysis. RNA was purified from intima-media specimens from valve and nonvalve areas that were either immediately frozen or cultured for 2 days. Single-read sequencing was carried out to generate approximately 10 million reads per sample. Differentially expressed genes and Gene Ontology (GO) terms that were over-represented or under-represented by the differentially expressed genes in the valve and day comparisons were determined.[17]

RESULTS

Increased SMC migration and proliferation in tissue explants of the valve sinus wall. SMCs from explants of the intima-media of the valve sinus wall (hereafter just called valve) migrate from explants 1 day sooner than SMCs from nonvalve intima-media. This was true for both the percentage of migration-positive explants (Fig 1, *A*, *left panel*) and the number of cells per explant (Fig 1, *A*, *right panel*). In contrast, the adventitial tissue explants showed no difference in the rate of migration of cells from valve vs nonvalve areas of the vein (Fig 1, *B*).

There were no significant differences between the valve and the nonvalve intima-media or adventitia in terms of cell density (Fig 2, *A*, *left and right panels*, respectively) or cell death (terminal deoxynucleotidyl transferase dUTP nick end labeling staining; Fig 2, *B*, *left and right panels*, respectively) in response to the injury of tissue dissection.

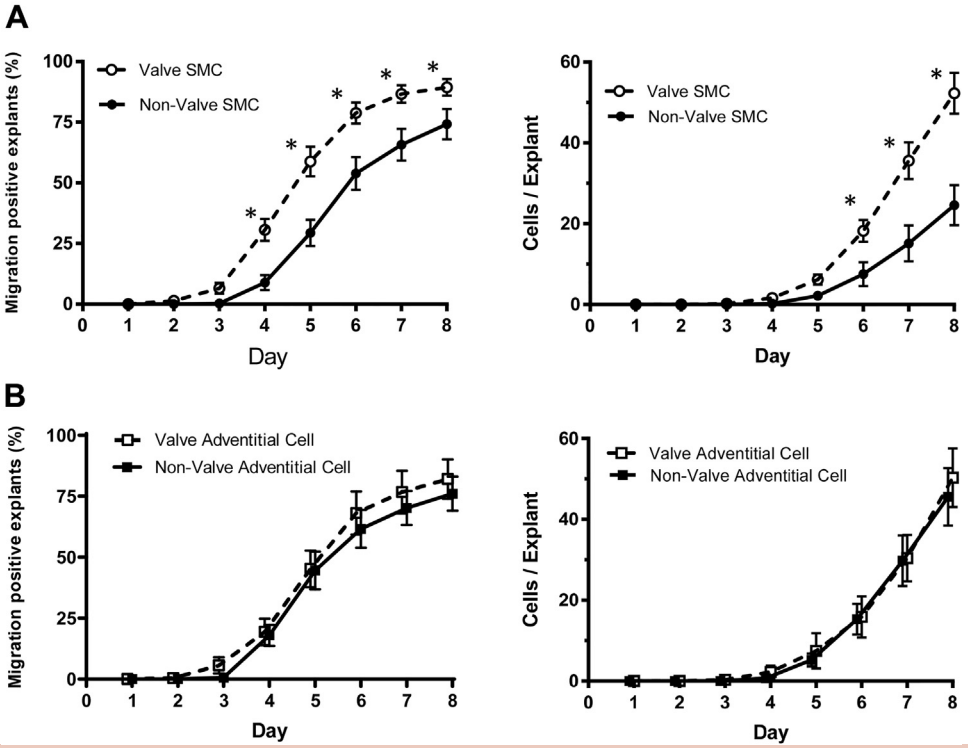

Fig 1. Valve smooth muscle cells (*SMCs*) from intimal-medial explants migrate more than nonvalve SMCs. Cell migration from the valve sinus (hereafter just called valve) compared with the nonvalve intimal-medial explants **(A)** or adventitial explants **(B).** Migration is presented as the percentage of migration-positive explants (one or more cells/explant, which measures only migration, *left panels*) and as the number of cells per explant (which measures a combination of migration and postmigration proliferation, *right panels*). *$P < .001$ paired valve vs nonvalve; n = 24 and 16 different veins for **A** and **B,** respectively.

However, SMC proliferation was higher by 4 days in the valve intima-media compared with the nonvalve intima-media (Ki67 staining; Fig 2, *C*, *left panel*). There was no difference in cell proliferation in the valve vs nonvalve adventitia (Fig 2, *C*, *right panel*). Thus, valve SMCs show increased rates of migration from tissue and proliferation in tissue in response to the injury of dissection and culture. Our subsequent studies focused on the intima-media tissue and their SMCs because there was no valve effect on the adventitia.

Cultured valve SMCs also migrate and proliferate faster than nonvalve SMCs. To determine if the increased migratory activity of valve SMCs is a stable phenotype, we studied cultured SMCs derived from valve and nonvalve segments, at passage 6. There were no statistically significant differences in the general SMC phenotype of valve vs nonvalve cells, as measured by a wide variety of parameters: expression of smooth muscle α-actin or smooth muscle myosin heavy chain by immunofluorescence (Fig 3, *A-C*); messenger RNA expression of smooth muscle α-actin (*ACTA2*), smooth muscle myosin heavy chain (*MYH11*), caldesmon 1 (*CALD1*), or NG2 (*CSPG4*; Fig 3, *D*). We found that valve SMCs migrated ~60% faster than nonvalve SMCs in response to both platelet-derived growth factor (PDGF) subunit BB (PDGF-BB) and 10% serum (Fig 4, *A*). The increased migration in response to PDGF-BB was due to increased chemotactic activity because the difference between valve SMCs and nonvalve SMCs was not observed when PDGF was placed in both the top and bottom chambers (Fig 4, *B*). In contrast, in response to serum, the increased migration by valve SMCs was due to increased chemokinetic activity (Fig 4, *C*). This difference was not due to differences in attachment to the polymeric collagen used for the migration assay as attachment was the same for both types of SMCs (Fig 4, *D*).

Proliferation of valve SMCs was also greater than that of nonvalve SMCs in response to PDGF-BB (Fig 5, *A*). In contrast, proliferation in response to 1% to 10% serum or to a commercial SMC growth medium that contains 5% fetal bovine serum and unknown amounts of fibroblast growth factor 2 (FGF2), epidermal growth factor, insulin, and heparin was no different between valve and nonvalve SMCs (Fig 5, *B* and *C*).

FGF2 is required for the increased migration and proliferation of cultured valve SMCs. We previously reported that PDGF-mediated proliferation of human arterial SMCs is partially mediated through the release of

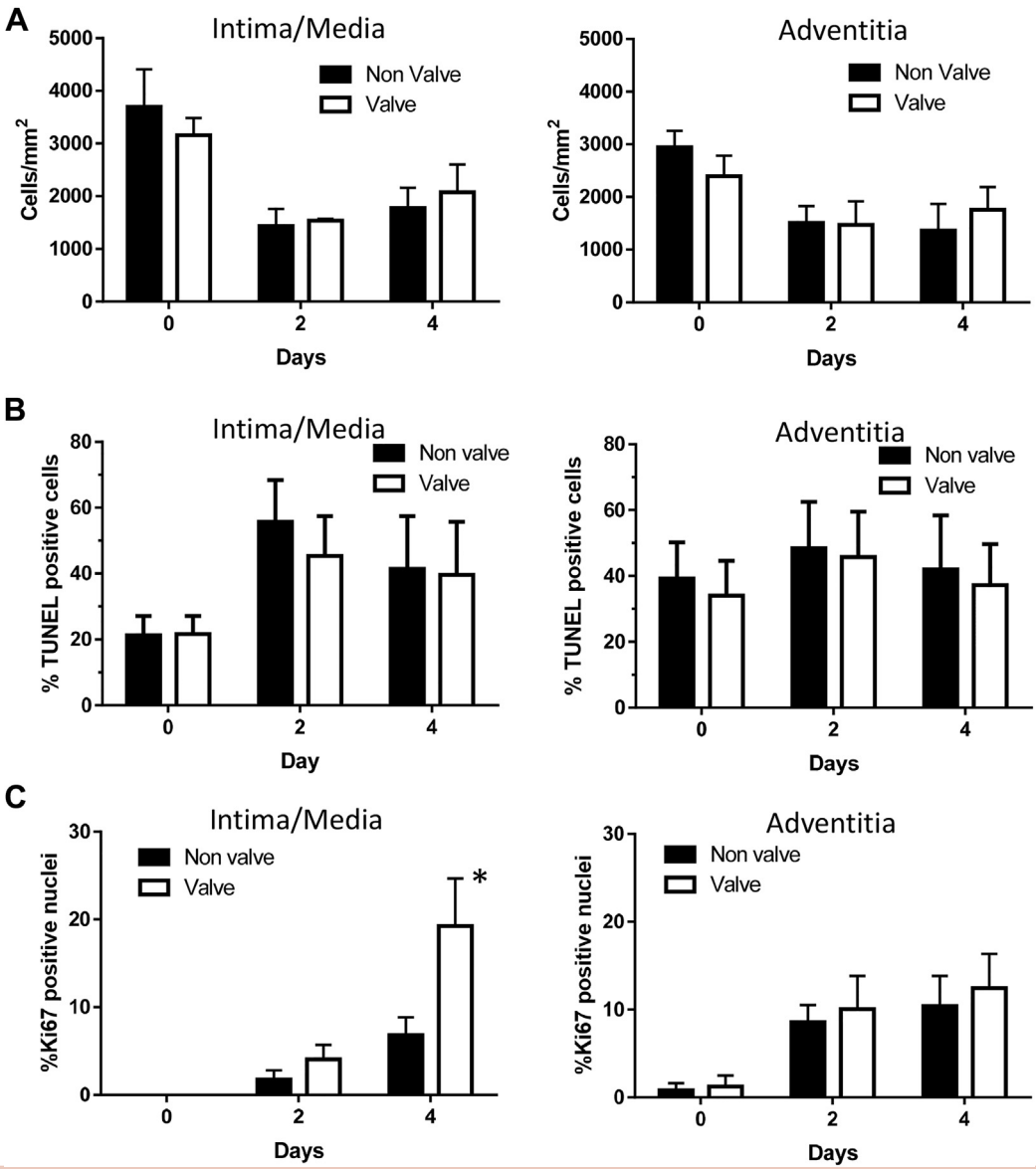

Fig 2. Valve smooth muscle cells (SMCs) proliferate more than nonvalve SMCs in response to injury. Cell density (**A,** cells/mm^2), death (**B,** % terminal deoxynucleotidyl transferase dUTP nick end labeling [*TUNEL*]-positive cells), and proliferation (**C,** % Ki67-positive nuclei) in intima-media (*left panels*) vs adventitia (*right panels*) of valve and nonvalve wall in response to tissue dissection and culture during 4 days. *$P < .05$ paired valve vs nonvalve; n = 4 veins.

pericellular, heparin-releasable, endogenous FGF2.[18] Therefore, we hypothesized that PDGF mediates valve SMC migration and proliferation because of increased heparin-sensitive FGF2 in valve SMCs. However, we found no difference in the amount of FGF2 in the heparin-releasable fraction, medium, or cell layer in valve and nonvalve SMCs before or after treatment with PDGF-BB (Supplementary Fig 2, *A*, online only). In addition, we found no difference in the relative amounts of the 18-kD, 22-kD, and 28-kD FGF2 isoforms, which can have different activities (Supplementary Fig 2, *B*, online only).[19] Although FGF2 levels were the same for valve and nonvalve SMCs, we found that blockade of FGF2 with FGF2 antibody inhibited most of the increased migration (Fig 6, *A*) and proliferation (Fig 6, *B*) of valve SMCs in response to PDGF-BB and did not change the migration or proliferation of nonvalve SMCs. Finally, valve but not nonvalve SMCs showed increased migration in response to FGF2 (Fig 6, *C*), indicating that FGF2 signaling is functional in valve SMCs but not in nonvalve SMCs. In combination, these data suggest that the FGF2 mechanisms mediating migration and proliferation are functional and operative in valve SMCs but not in the nonvalve SMCs.

We also observed another valve-specific effect regarding PDGF-BB-mediated migration. Anti-PDGF receptor (PDGFR) β only partially inhibited the PDGF-BB-induced

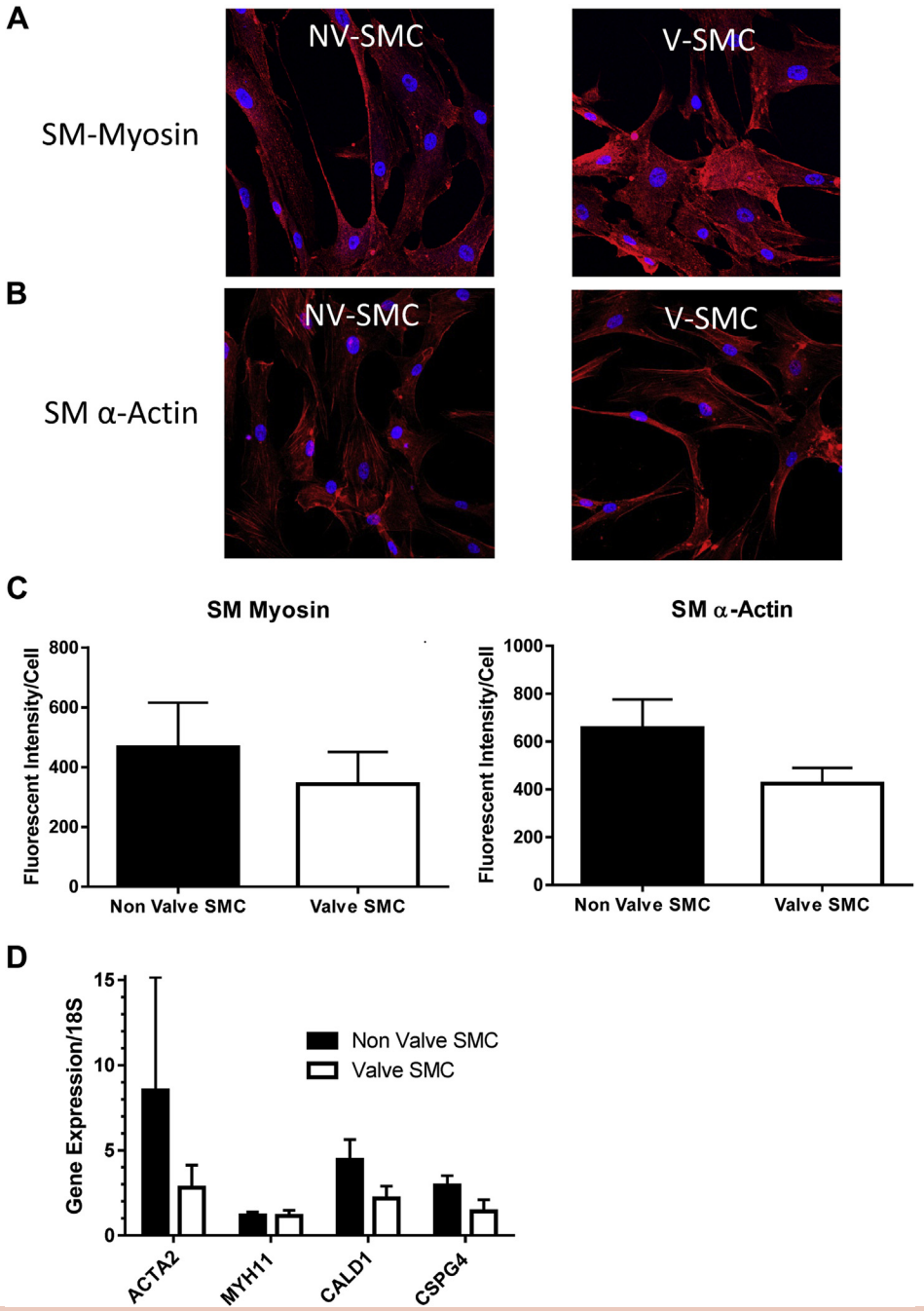

Fig 3. Valve (*V-SMC*) and nonvalve (*NV-SMC*) smooth muscle cells (*SMCs*) have equivalent expression of SMC markers. Representative immunofluorescent staining for **(A)** smooth muscle myosin heavy chain (*SM-Myosin*) and **(B)** smooth muscle α-actin (*SM-α-actin*) in valve and nonvalve SMCs was quantified for five pairs of valve and nonvalve SMCs **(C). D,** Levels of SMC marker messenger RNA in valve and nonvalve SMCs: smooth muscle α-actin (*ACTA2*), smooth muscle myosin heavy chain (*MYH11*), caldesmon 1 (*CALD1*), and NG2 (*CSPG4*); n = 4 pairs of valve and nonvalve SMCs.

migration of valve SMCs (Supplementary Fig 3, *A*, *left panel*, online only) but completely blocked nonvalve SMC migration. Using a combination of maximally effective anti-PDGFRα and PDGFRβ also did not completely block the effect of PDGF-BB in the valve SMCs (Supplementary Fig 3, *B*, online only), whereas a combination of anti-FGF2 and anti-PDGFRβ inhibited PDGF-BB-mediated valve SMC migration >90% (Supplementary Fig 3, *C*, online only).

The inability to completely block PDGF-BB-mediated migration in the valve SMCs with the combination of anti-PDGFRα and anti-PDGFRβ was surprising because

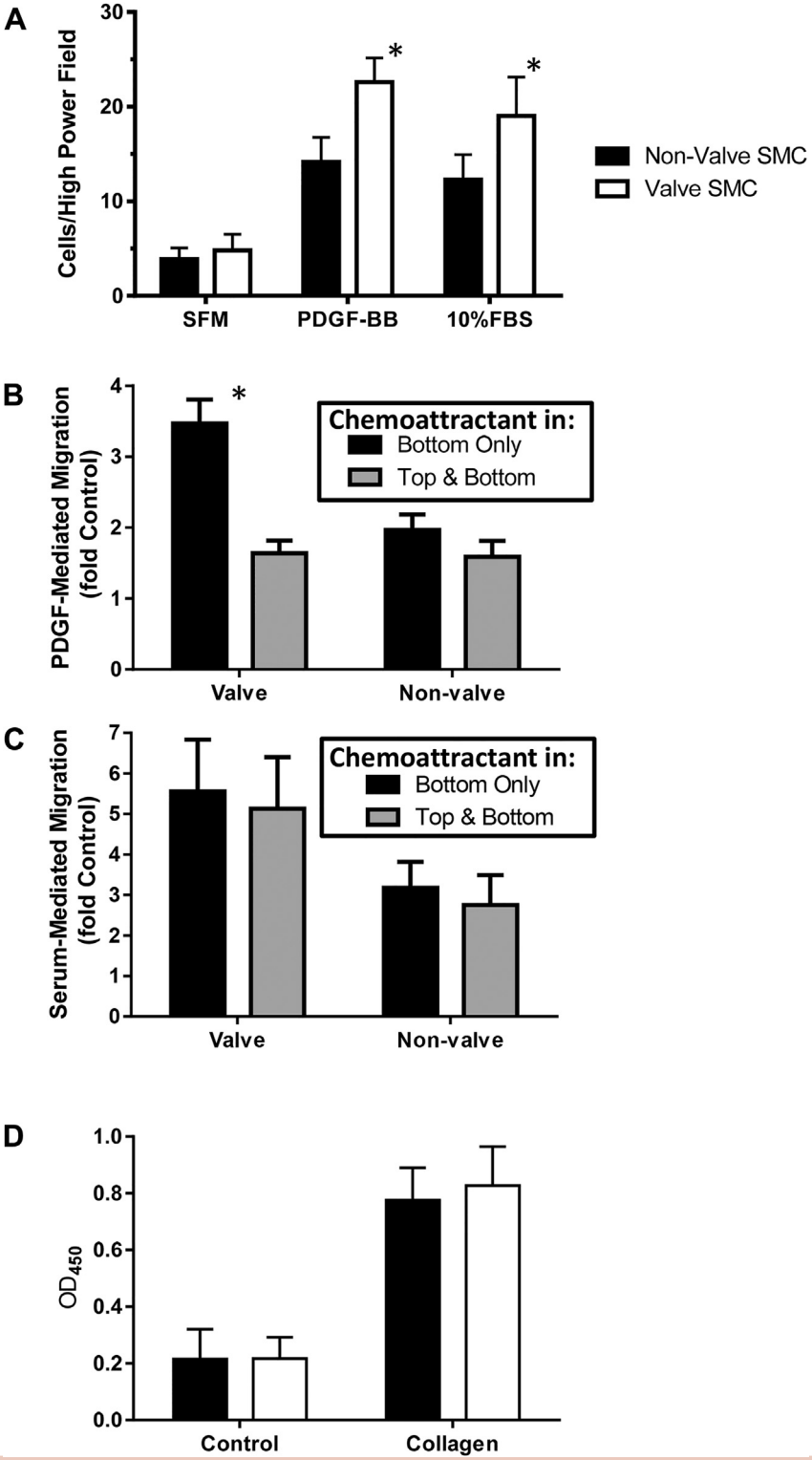

Fig 4. Valve smooth muscle cells (*SMCs*) show increased chemotactic migration to platelet-derived growth factor subunit BB (*PDGF-BB*) and increased chemokinetic migration to serum. Valve and nonvalve SMC migration was measured using a microchemotaxis chamber assay. **A,** Migration in response to PDGF-BB or 10% fetal bovine serum (*FBS*). *$P < .01$ valve vs nonvalve; results are from paired cells from seven veins. *SFM,* Serum-free medium. **B** and **C,** Valve and nonvalve SMC migration was determined in microchemotaxis chambers with either 10 ng/mL PDGF-BB **(B)** or 10% serum **(C)** in only the bottom chamber or in both top and bottom chambers. *$P < .01$ top only vs top and bottom; n = 5 experiments. **D,** Attachment of SMCs to polymeric collagen measured using the crystal violet assay; n = 4 experiments. *OD,* Optical density.

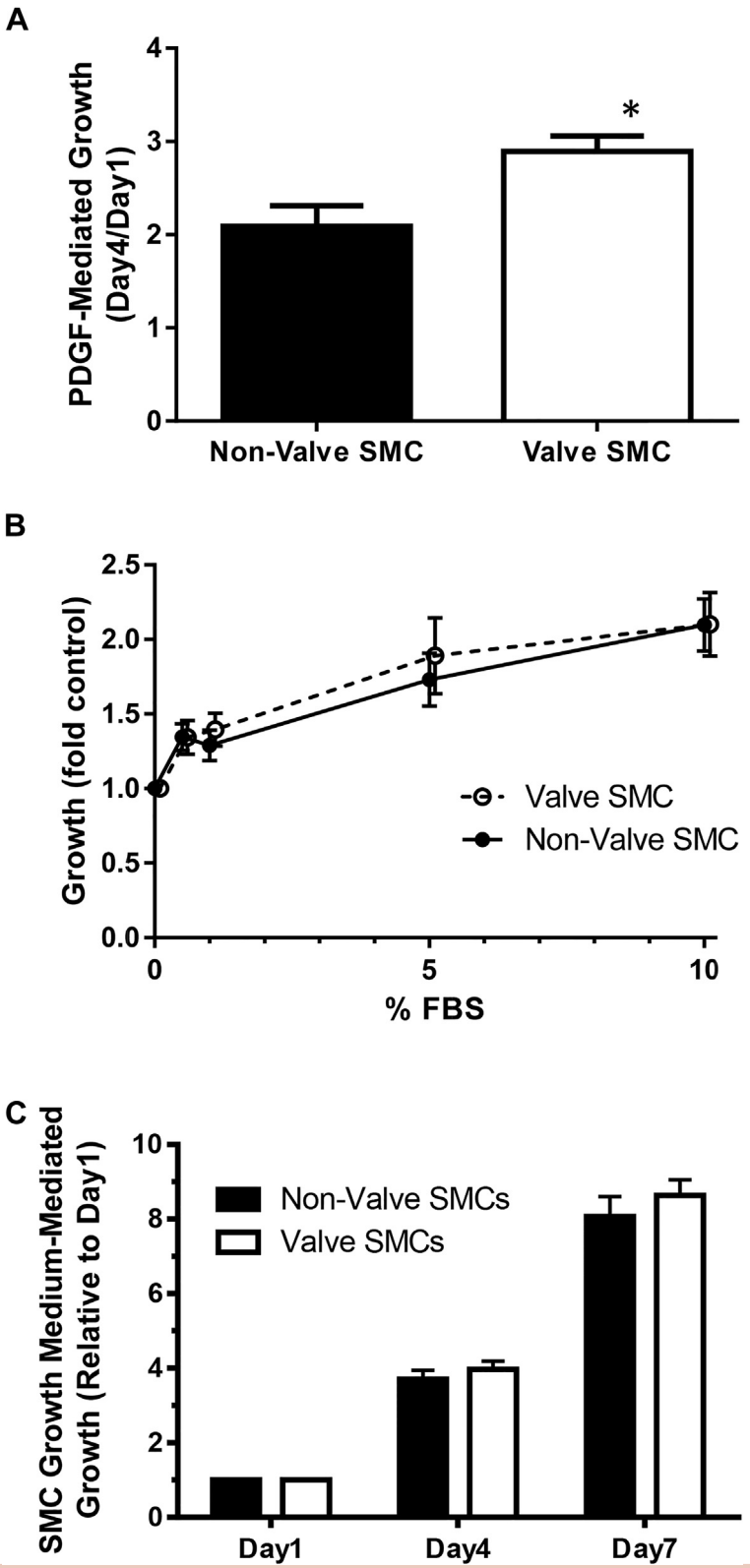

Fig 5. Valve smooth muscle cell (*SMC*) proliferation is stimulated differentially by platelet-derived growth factor (*PDGF*) subunit BB (PDGF-BB). Proliferation of valve vs nonvalve SMCs in response to PDGF-BB + 2% serum **(A),** 1% to 10% serum **(B),** or a commercial SMC growth medium **(C)**. *FBS*, Fetal bovine serum. Results are presented as the mean ratio (±standard error of the mean) of day 4 to day 1 cell counts or as fold of control. *$P < .05$ valve vs nonvalve; n = 5, 6, or 9 pairs of cells for **A, B,** and **C,** respectively.

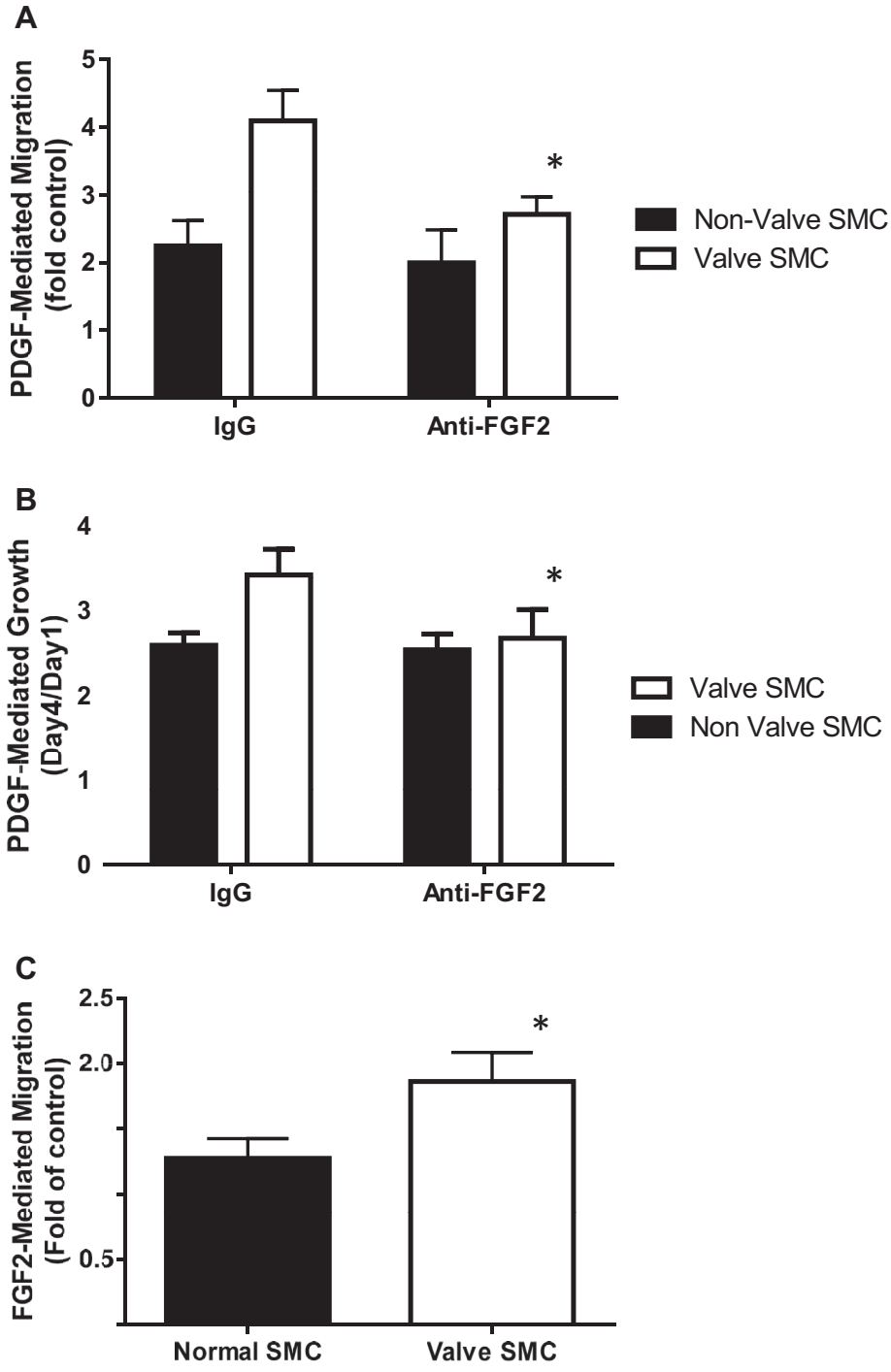

Fig 6. Fibroblast growth factor 2 (*FGF2*) antibody blocks increased platelet-derived growth factor (*PDGF*) subunit BB (PDGF-BB)-induced valve smooth muscle cell (*SMC*) migration and proliferation. The effect of a blocking antibody to FGF2 on valve vs nonvalve SMC migration (microchemotaxis chamber, **A**) and proliferation **(B)** mediated by 10 ng/mL PDGF-BB. Results are presented as fold of control in **A** and as the ratio (±standard error of the mean) of day 4 to day 1 cell counts in **B.** **P* < .05 anti-FGF2 vs immunoglobulin G (*IgG*) control; n = 5-7 pairs of cells. **C,** The effect of exogenous FGF2 (10 ng/mL) on migration of valve and nonvalve SMCs in a chemotaxis chamber assay. **P* = .003 FGF2 vs unstimulated control; n = 5 different pairs of valve and nonvalve SMCs.

the established receptors for PDGF-BB are PDGFRβ and PDGFRα. To confirm this observation, we tested them using a different migration assay. In the scratch assay, the effect of PDGF-BB was completely blocked by the PDGFRβ antibody in both valve and nonvalve SMCs (Supplementary Fig 4, online only). In addition, the antibody to FGF2 still completely blocked migration of valve SMCs but had no effect on nonvalve SMCs, thus

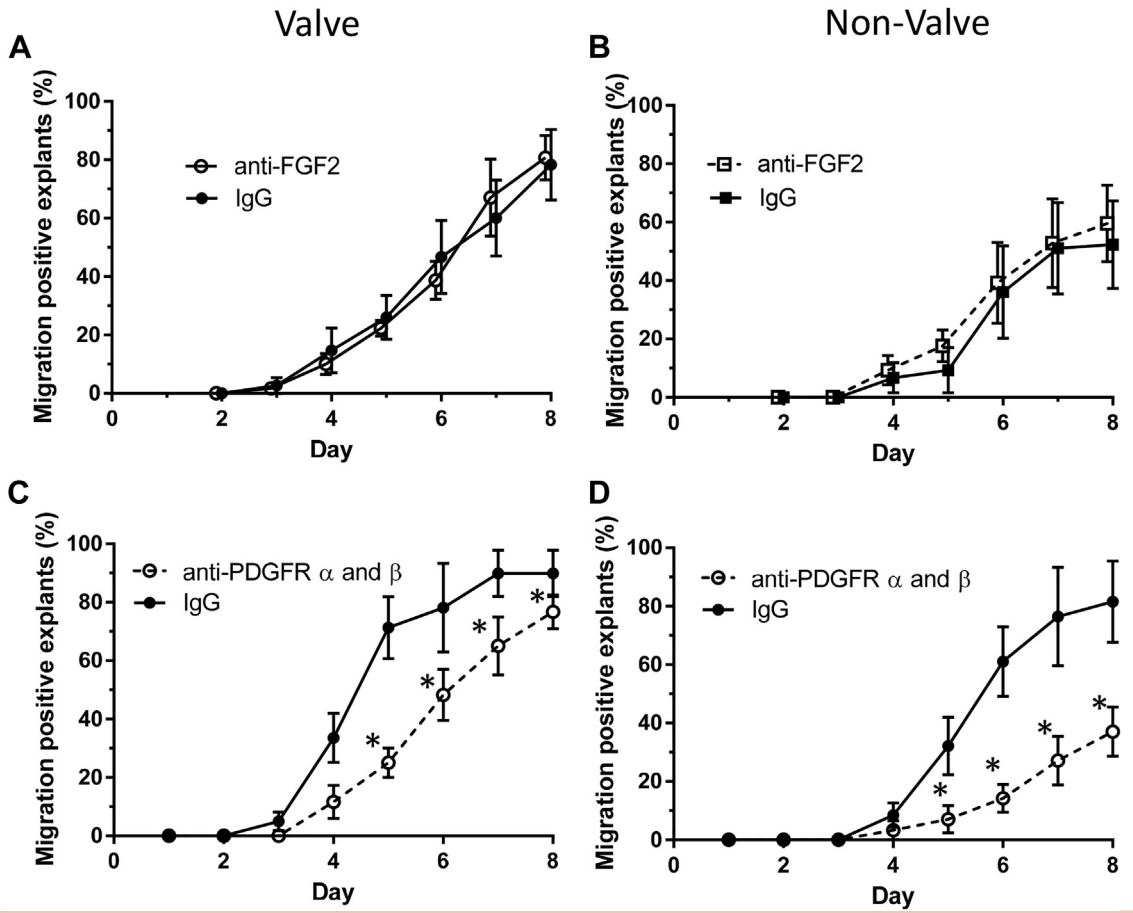

Fig 7. Migration from explants is not affected by anti-fibroblast growth factor 2 (*FGF2*), and platelet-derived growth factor receptor (*PDGFR*) blockade is more effective in nonvalve smooth muscle cells (SMCs). The effect of the blocking antibody to FGF2 (or goat immunoglobulin G [*IgG*]; both at 60 μg/mL) on SMC migration from valve **(A)** and nonvalve **(B)** intimal-medial tissue (n = 5 veins). The effect of a combination of antibodies to PDGFR α and β (5 μg/mL each or 10 μg/mL mouse IgG) on SMC migration from valve **(C)** and nonvalve **(D)** intimal-medial tissue (*$P < .01$ vs IgG; n = 4 veins). Migration is presented as mean migration-positive explants (one or more cells migrating from explant).

demonstrating valve SMC specificity for FGF2 in both migration assays. However, there was no difference in migration between valve SMCs and nonvalve SMCs, the level of which was less than seen in the chemotaxis chamber assay (for valve SMCs, 1.5-fold increase in the scratch vs >4-fold with the microchemotaxis assay; Supplementary Fig 4, online only, vs Fig 4, *A*). This may be because the increased migration of valve SMCs in response to PDGF results from chemotaxis (Supplementary Fig 4, online only), and there is no chemotactic gradient in the scratch assay.

To summarize, these data indicate that both FGF2 and PDGFRβ are required for the full PDGF-BB-mediated migratory response of cultured valve SMCs, whereas FGF2 is not required by nonvalve SMCs.

FGF2 blockade does not alter SMC migration from tissue explants. To see if these growth factor mechanisms found in cell culture also functioned in the more complex tissue explants, we tested the effect of blockade of FGF2 on the migration of SMCs from valve intimal-medial explants. PDGF and FGF2 are known to mediate SMC migration in vivo.[20,21] Unexpectedly, blockade of FGF2 did not alter migration of SMCs from either valve or nonvalve intimal-medial explants (Fig 7, *A* and *B*, respectively). A combination of antibodies to PDGFR α and β, as expected, inhibited SMC migration from both valve (Fig 7, *C*) and nonvalve (Fig 7, *D*) tissue explants. Thus, unlike the behavior of the cells cultured from the explants, neither FGF2 nor PDGFRs mediated *augmented* migration of valve SMCs from tissue explants, leaving open the question of what is involved in the more complex tissue.

Differential gene expression in valve vs nonvalve tissue. To determine possible mediators of the increased migration of valve SMCs, we measured global gene expression in valve and nonvalve intimal-medial tissue.

Table. Differentially expressed genes in valve vs nonvalve intimal-medial tissue

Significant valve vs nonvalve genes		Valve vs nonvalve log fold change	FDR
BRINP3	Bone morphogenetic protein/retinoic acid inducible neural-specific protein	4.52	0.008
NTS	Neurotensin	4.22	0.006
BATF	Basic leucine zipper transcription factor, ATF-like	3.90	0.000
PROX1	Prospero homeobox 1	3.70	0.000
TMEM100	Transmembrane protein 100	3.21	0.017
OAF	OAF homolog (*Drosophila*)	3.15	0.000
MMP10	Stromelysin 2	3.10	0.000
SEMA3A	Semaphorin 3A	2.98	0.008
PIK3C2G	Phosphatidylinositol-4-phosphate 3-kinase, catalytic subunit type 2	2.72	0.000
GATA3	GATA binding protein 3	2.46	0.000
GATA3-AS1	GATA binding protein 3-antisense 1	2.29	0.003
PAPPA2	Pappalysin 2	2.28	0.032
DSP	Desmoplakin	2.27	0.009
PTH2R	Parathyroid hormone 2 receptor	2.19	0.001
ADAMTSL2	ADAMTS-like 2	2.18	0.003
HRH2	Histamine receptor H2	2.13	0.008
PLCXD3	Phosphatidylinositol-specific phospholipase C, X domain containing3	1.49	0.009
KRT7	Keratin 7	1.46	0.008
PLA2G2A	Phospholipase A_2, group IIA	1.40	0.010
PKHD1L1	Polycystic kidney and hepatic disease 1 (autosomal recessive)-like	1.28	0.008
UBXN10	UBX domain protein 10	1.09	0.053
C6	Complement component 6	0.90	0.016
C7	Complement component 7	−0.50	0.043
MBP	Myelin basic protein	−1.18	0.053
MT-ND1	Mitochondrially encoded NADH dehydrogenase 1	−1.42	0.052
MT-ND5	Mitochondrially encoded NADH dehydrogenase 5	−1.43	0.009
CDH2	Cadherin 2, type 1, N-cadherin (neuronal)	−1.46	0.010
TPH1	Tryptophan hydroxylase 11	−1.81	0.011
Significant time-valve interaction genes		**Tissue-time interaction log fold change**	
SNHG15	Small nucleolar RNA host gene 15 (non-protein coding)	3.50	0.050
LINC01272	Long intergenic non-protein coding RNA	−2.54	0.051
C2CD4A	C2 calcium-dependent domain containing 4A	4.15	0.051
SALL1	Spalt-like transcription factor 1	1.74	0.051
IQCA1	IQ motif containing with AAA domain 1	−1.06	0.051
KIT	Stem cell factor receptor	2.91	0.051
PCDH12	Protocadherin 12	3.11	0.051
KCNQ1	Potassium voltage-gated channel, KQT-like subfamily, member 1	1.89	0.051
PCDHB19P	Protocadherin beta 19 pseudogene	3.50	0.050

AAA, ATPases associated with diverse cellular activities; *FDR*, false discovery rate; *NADH*, reduced form of nicotinamide adenine dinucleotide.

Freshly dissected tissue (with endothelium and valve leaflets removed) was compared with tissue cultured for 2 days. This time frame was chosen because cells begin to migrate from tissue at day 3 (Fig 1).

We found 31 genes that were differentially expressed in valve compared with nonvalve tissue, and 6 genes were differentially expressed in the interaction between tissue type and time (Table; Supplementary Table I, online only). GO analysis of significant valve vs nonvalve genes yielded the categories of immune response, regulation of inflammatory response, development, and response to wounding (Supplementary Table II, online only). Analysis of significant tissue type and time interaction genes yielded four different categories of development

(Supplementary Table III, online only). Protein-protein interaction analysis (STRING database) of the differentially expressed genes indicated that a higher number of interactions (seven) exist among these genes than would be expected by chance ($P = .03$; Supplementary Fig 5, online only).

Valve-specific inhibitory effect of *SEMA3A* on SMC migration from tissue explants. We chose *SEMA3A* to test (Table; Supplementary Table IV, online only) because it has been shown, along with its receptor NRP1, to be required for lymphatic valve development and to alter cell migration. Also, it is a soluble factor with characterized inhibitory reagents.[22-24] We used a peptide that competes with the immunoglobulin domain of *SEMA3A* for binding to NRP1 (SEMApeptide) and a peptide that competes with the MAM domain of NRP1 that mediates NRP1 dimerization (MAMpeptide; Fig 8, *A*). Both of these peptides block the neural growth cone collapse activity of *SEMA3A*.[25] Blockade of *SEMA3A* with the *SEMA3A* peptide increased the number of cells per explant (measures the combination of migration and post-migration proliferation) in valve but not in nonvalve explants (Fig 8, *B*, *left and right panels*, respectively). In contrast, the MAMpeptide decreased the number of cells per explant in valve *and* in nonvalve explants. There was no significant effect of either peptide on the number of migration-positive explants (Fig 8, *C*), although the trends were the same. These data demonstrate a valve-specific stimulatory effect for the *SEMA3A* peptide, which indicates that *SEMA3A* is a valve-specific SMC migration inhibitor. There was an inhibitory effect of the MAMpeptide, which indicates that NRP1 stimulates SMC migration in both valve and nonvalve tissue. Thus, these data demonstrate a novel inhibitory role for *SEMA3A* in human venous valves but do not provide an explanation for the increased response to injury of the valve SMCs.

DISCUSSION

This study presents the novel observation that SMCs but not adventitial cells from the valve sinus region of human saphenous veins demonstrate more vigorous proliferation and migration in response to the injury of tissue disruption or when stimulated by PDGF or serum in culture than those from areas adjacent to the valve sinus. The explant response to injury closely parallels the time courses of cell proliferation and migration seen after vascular injury in vivo. Baboon, rat, and mouse arteries injured in vivo and baboon arterial medial explants ex vivo show entry into the cell cycle at 2 or 3 days and migration at 3 or 4 days after injury.[14,26,27] In comparison, the lag times for entry into the cell cycle of human saphenous vein explant SMCs and for SMC migration from tissue were 2 days and 3 or 4 days, respectively.

Mechanisms and growth factors. The augmented migration and proliferation of cultured valve SMCs compared with nonvalve SMCs in response to PDGF-BB is mediated by FGF2. Exogenous FGF stimulated and an FGF2 blocking antibody inhibited migration and proliferation of valve SMCs but not of nonvalve SMCs. Our data also suggest that the actions of PDGF-BB on valve SMCs require pathways outside of the classic PDGF receptors, PDGFRα and PDGFRβ. We were unable to completely inhibit PDGF-BB-mediated migration of valve SMCs in the microchemotaxis chamber assay using maximal doses of the PDGFR blocking antibodies, whereas blockade of PDGFRβ completely blocked migration of valve SMCs in the scratch assay. In contrast, blockade of PDGFRβ completely blocked migration of nonvalve SMCs in both assays. However, concomitant blockade of PDGFRβ and FGF2 completely blocked valve SMC migration in the chemotaxis assay (Supplementary Fig 3, *C*, online only). This suggests the possibility of a PDGF receptor beyond PDGFRα and PDGFRβ in the valve SMCs or another pathway that is operative only in the chemotaxis assay. In this regard, Pellet-Many et al[28] found an inhibitory effect of the cytoplasmic deletion mutant of NRP1 on PDGF-mediated SMC migration in the Transwell system (Fisher Scientific, Waltham, Mass) but not in the scratch assay. The Transwell system, unlike the scratch assay, develops a chemotactic gradient. Banerjee et al[29] reported that PDGF-BB binds to NRP1 and suggested that this may mediate effects of PDGF-BB on SMC migration. FGF2 has also been shown to bind to NRP1, which potentiates the growth-promoting activity of FGF2.[30] Thus, it is possible that in valve SMCs, NRP1 may mediate additional effects of both PDGF and FGF2 in a manner not involving PDGFRβ, which could explain the increased effect of PDGF-BB and the valve-specific effect of FGF2 in valve SMCs. Further experiments are needed to test this hypothesis.

In summary, the increased migration of cultured valve SMCs is mediated by a differential response to FGF2 by unknown mechanisms. In contrast, the increased migration of valve SMCs from tissue explants does not involve FGF2 but may be mediated by novel pathways involving some of the genes that are differentially expressed in valve tissue as highlighted by this study.

Valve wall gene expression. Consistent with differential expression, we found that the peptide with the *SEMA3A* sequence (SEMApeptide) had a valve-specific effect on SMC migration. However, it had a stimulatory effect. This suggests that *SEMA3A* is an inhibitor and so does not explain the increased migration of valve SMCs. Of interest in this regard, Movassagh et al[31] recently reported that *SEMA3A* inhibits the PDGF-mediated proliferation of cultured human airway SMCs, whereas Kutschera et al[32] reported no effect of *SEMA3A* on human umbilical artery SMC migration.

Other attractive candidates for valve stimulatory genes are the tyrosine kinase receptor *KIT* (stem cell factor

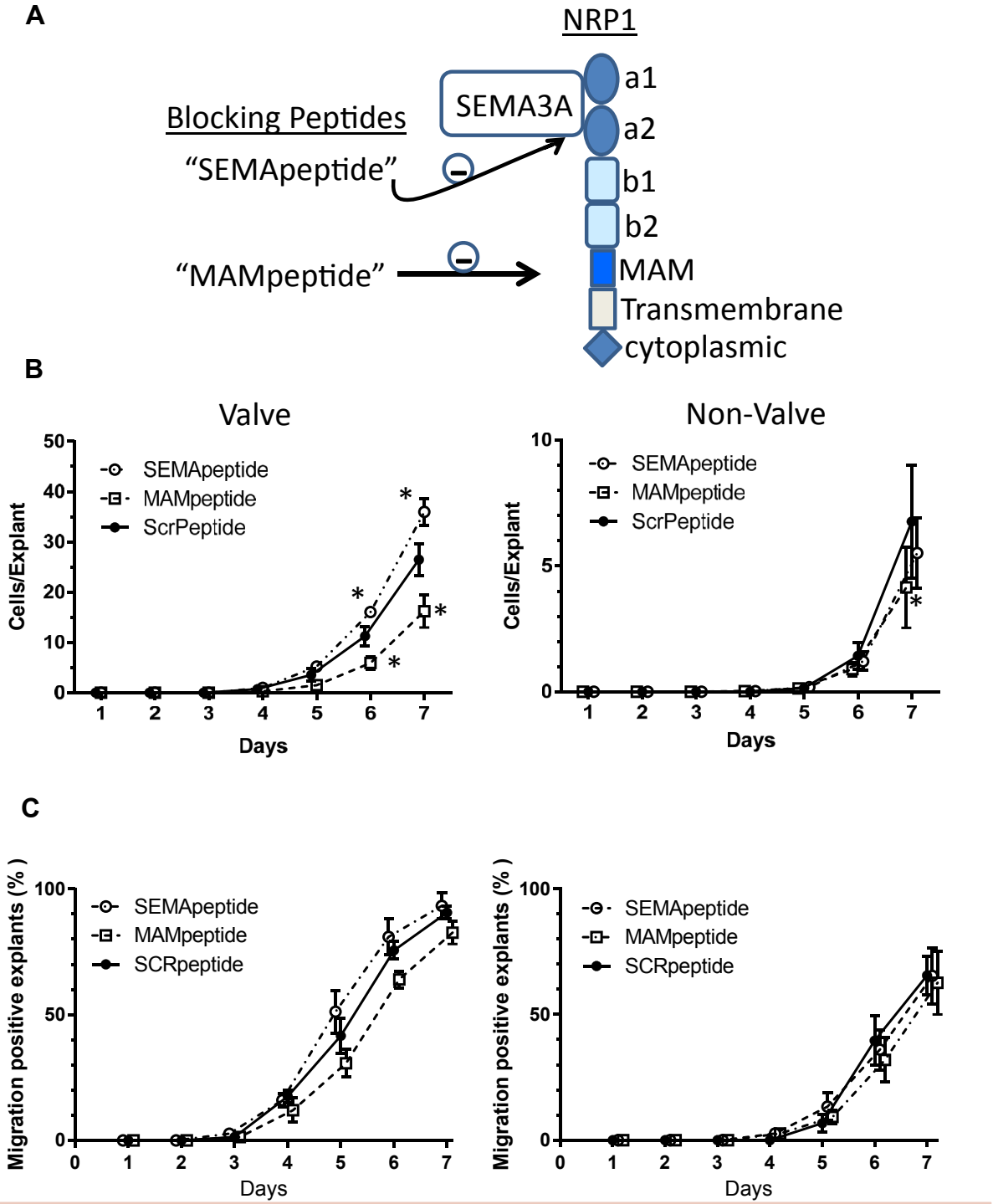

Fig 8. SEMApeptide selectively increases valve smooth muscle cell (SMC) migration from explants. **A,** Schematic of NRP1 structure with the blocking peptides used in this experiment. **B,** The effect of the SEMApeptide, MAMpeptide, or scrambled peptide (SCRpeptide), each at 20 μM on SMC migration/proliferation (cell number/explant) from valve (*left panel*) and nonvalve (*right panel*) intimal-medial tissue (*$P < .05$ vs SCRpeptide; n = 5 veins). **C,** The effect of the SEMApeptide, MAMpeptide, or scrambled peptide (SCRpeptide) on the percentage migration of positive explants (one or more cells migrating from explant) from valve (*left panel*) and nonvalve (*right panel*) intima-media (n = 5 veins).

receptor), *GATA3*, and N-cadherin (*CDH2*). *KIT* plays a positive role in vasculogenesis and injury-mediated intimal hyperplasia[33,34] and is more highly expressed in valve tissue. *GATA3* is required for tissue regeneration,[35] mediates SMC hyperplasia in lung injury models,[36] and is more highly expressed in valve tissue. Finally,

N-cadherin is an inhibitor of SMC proliferation and migration,[37] and levels of N-cadherin messenger RNA are significantly lower in valve tissue compared with nonvalve tissue. Further work is needed to identify the key stimulatory molecules in valve tissue.

The reactivation of developmental pathways after vascular injury has been known for many years (eg, Weiser-Evans et al[38]), so it is not surprising that more than half of the GO categories for differentially expressed genes involve development (Supplementary Table III, online only). The genes in these categories include *SALL1*, *KIT*, *TGFB3*, *KCNQ1*, *PCDH12*, *GATA3*, *PROX1*, *DSP*, *BATF*, *SEMA3A*, *HRH2*, *TMEM100*, *PLA2G2A*, and *BRINP3*. A number of genes are known to be required for venous valve formation, including the genes encoding FoxC2[39]; Connexins 37, 43, and 47[40]; and Ephrin B2, Prox1, and integrin α_9.[8] *PROX1* is a master gene of lymphatic development. It is required for differentiation of venous endothelial cells to lymphatic endothelial cells. FoxC2, EphrinB2, and Sema3A are required for lymphatic maturation, such as valve formation and SMC attachment.[22,41] However, each of these genes has been shown to be acting in venous endothelial cells. *PROX1* is the only one of these *venous* valve genes that is differentially expressed in the valve intimal-medial tissue. It is likely that endothelial cells are represented in our preparations of intimal-medial tissue because the vasa vasorum penetrates deep into the media of veins[42] (unpublished data). However, it is unlikely that there is a difference in the number of endothelial cells in valve vs nonvalve tissue because expression by RNA sequencing of typical endothelial cell markers (CD31, MSR1, von Willebrand factor, angiotensin-converting enzyme, CDH5 [endothelial cadherin, intercellular adhesion molecule 2, CD36, and endoglin) was not significantly different between the valve and nonvalve tissue. The higher expression of *PROX1* in valve compared with nonvalve explants may simply represent preferential expression of *PROX1* in the endothelial cells present in valve medial tissue.

Clinical implications. The observation of a greater response to injury by the valve wall segment has implications for vein graft failure, chronic venous insufficiency, and deep venous thrombosis, each of which represents a different injury to the venous wall (ie, arterial pulse pressure and flow, venous hypertension, and the local thromboinflammatory effects of a thrombus, respectively). Regarding arterial vein graft failure, 8% to 18% of lesions occur at valve sites.[4-7] In the case of reversed vein grafts, most of the valve leaflets become fibrotic, which may result from the greater migratory and proliferative phenotype of the valve SMC.

Regarding venous thrombosis, the valve sinus is often the site of thrombus initiation and has been reported to express less fibrinolytic activity.[43] Activated platelets in the thrombus release the contents of their granules, which include PDGF. Our data indicate that SMCs in the valve sinus have a greater migratory and proliferative response to PDGF than do the nonvalve SMCs, which could lead to greater wall thickening in the valve area. In turn, this thickening of the vein, by vessel remodeling or luminal encroachment, may then lead to valve dysfunction, as has been suggested for the valve and wall thickening observed with increasing age.[1,44,45] Increased valve SMC activation, particularly the immune and inflammatory pathways indicated by our GO results (Supplementary Tables II and III, online only), may also contribute to the thrombotic response. A link between venous thrombosis, sterile inflammation, and the innate immune response has been suggested as TLR9 knockout mice had larger venous thrombi than wild-type mice.[46] A further link between immune function and venous injury is that long-term vein bypass graft failure has been associated with single-nucleotide polymorphisms in complement component (3b/4b) receptor 1, MICA, and HLA-DPB1, the last two of which are human leukocyte antigen class I and class II major histocompatibility complex components, respectively.[47] Finally, the SMCs of experimental vein grafts show inflammatory activation.[48] This study is significant in that the GO results demonstrate that the valve wall further increases the activities of these immune/inflammation pathways. Whether this plays a role in post-thrombotic syndrome, which occurs in ~30% of patients with deep venous thrombosis,[3] or chronic venous insufficiency is not clear and could not be studied in the current work because of the difficulty of obtaining histologic specimens. This limitation in our methodology cannot be replaced by animal models as they lack venous valves.[49]

CONCLUSIONS

SMCs of the valve sinus exhibit an exaggerated response to injury compared with SMCs of the nonvalve wall, which may explain the propensity of the valve wall to fail in arterial bypass grafts and for the valves to fail after thrombotic events.

We thank Drs Mark Hill (Virginia Mason Hospital, Seattle, Wash) and Ted Kohler (Division of Vascular Surgery, VA Puget Sound Health Care System, University of Washington) for procuring veins.

AUTHOR CONTRIBUTIONS

Conception and design: SK, RK
Analysis and interpretation: SK, LC, YS, NA, GT, MS, TW, RK
Data collection: SK, LC, KX, YS, RK
Writing the article: RK
Critical revision of the article: SK, LC, KX, YS, NA, GT, MS, TW, RK
Final approval of the article: SK, LC, KX, YS, NA, GT, MS, TW, RK

Statistical analysis: SK, RK
Obtained funding: SK, MS, RK
Overall responsibility: RK

REFERENCES

1. Eberhardt RT, Raffetto JD. Chronic venous insufficiency. Circulation 2014;130:333-46.
2. Mackman N. New insights into the mechanisms of venous thrombosis. J Clin Invest 2012;122:2331-6.
3. Ten Cate-Hoek AJ, Henke PK, Wakefield TW. The post thrombotic syndrome: ignore it and it will come back to bite you. Blood Rev 2016;30:131-7.
4. Vesti BR, Primozich J, Bergelin RO, Strandness E Jr. Follow-up of valves in saphenous vein bypass grafts with duplex ultrasonography. J Vasc Surg 2001;33:369-74.
5. Szilagyi DE, Elliott JP, Hageman JH, Smith RF, Dall'olmo CA. Biologic fate of autogenous vein implants as arterial substitutes. Ann Surg 1973;178:232-45.
6. Mills JL, Fujitani RM, Taylor SM. The characteristics and anatomic distribution of lesions that cause reversed vein graft failure: a five-year prospective study. J Vasc Surg 1993;17:195-204; discussion: 204-6.
7. Tullis MJ, Primozich J, Strandness DE Jr. Detection of "functional" valves in reversed saphenous vein bypass grafts: identification with duplex ultrasonography. J Vasc Surg 1997;25:522-7.
8. Bazigou E, Lyons OT, Smith A, Venn GE, Cope C, Brown NA, et al. Genes regulating lymphangiogenesis control venous valve formation and maintenance in mice. J Clin Invest 2011;121:2984-92.
9. George SJ, Johnson JL, Smith MA, Jackson CL. Plasmin-mediated fibroblast growth factor-2 mobilisation supports smooth muscle cell proliferation in human saphenous vein. J Vasc Res 2001;38:492-501.
10. George SJ, Johnson JL, Smith MA, Angelini GD, Jackson CL. Transforming growth factor-β is activated by plasmin and inhibits smooth muscle cell death in human saphenous vein. J Vasc Res 2005;42:247-54.
11. Owens CD, Gasper WJ, Rahman AS, Conte MS. Vein graft failure. J Vasc Surg 2015;61:203-16.
12. Kenagy RD, Clowes AW, Greenhalgh RM, Powell JT. Proliferation response after angioplasty. In: Greenhalgh RM, Powell JT, editors. Inflammatory and thrombotic problems in vascular surgery. Philadelphia: WB Saunders; 1997. p. 257-66.
13. Kenagy RD, Hart CE, Stetler-Stevenson WG, Clowes AW. Primate smooth muscle cell migration from aortic explants is mediated by endogenous platelet-derived growth factor and basic fibroblast growth factor acting through matrix metalloproteinases 2 and 9. Circulation 1997;96:3555-60.
14. Kenagy RD, Vergel S, Mattsson E, Bendeck M, Reidy MA, Clowes AW. The role of plasminogen, plasminogen activators, and matrix metalloproteinases in primate arterial smooth muscle cell migration. Arterioscler Thromb Vasc Biol 1996;16:1373-82.
15. Kenagy RD, Clowes AW. Blockade of smooth muscle cell migration and proliferation in baboon aortic explants by interleukin-1β and tumor necrosis factor-α is nitric oxide-dependent and nitric oxide-independent. J Vasc Res 2000;37:381-9.
16. Kenagy RD, Civelek M, Kikuchi S, Chen L, Grieff A, Sobel M, et al. Scavenger receptor class A member 5 (SCARA5) and suprabasin (SBSN) are hub genes of coexpression network modules associated with peripheral vein graft patency. J Vasc Surg 2016;64:202-9.e6.
17. Young MD, Wakefield MJ, Smyth GK, Oshlack A. Gene ontology analysis for RNA-seq: accounting for selection bias. Genome Biol 2010;11:R14.
18. Millette E, Rauch BH, Defawe O, Kenagy RD, Daum G, Clowes AW. Platelet-derived growth factor-BB-induced human smooth muscle cell proliferation depends on basic FGF release and FGFR-1 activation. Circ Res 2005;96:172-9.
19. Chlebova K, Bryja V, Dvorak P, Kozubik A, Wilcox WR, Krejci P. High molecular weight FGF2: the biology of a nuclear growth factor. Cell Mol Life Sci 2009;66:225-35.
20. Jackson CL, Raines EW, Ross R, Reidy MA. Role of endogenous platelet-derived growth factor in arterial smooth muscle cell migration after balloon catheter injury. Arterioscler Thromb 1993;13:1218-26.
21. Jackson CL, Reidy MA. Basic fibroblast growth factor: its role in the control of smooth muscle cell migration. Am J Pathol 1993;143:1024-31.
22. Bouvree K, Brunet I, Del Toro R, Gordon E, Prahst C, Cristofaro B, et al. Semaphorin3A, Neuropilin-1, and PlexinA1 are required for lymphatic valve formation. Circ Res 2012;111:437-45.
23. Nasarre C, Koncina E, Labourdette G, Cremel G, Roussel G, Aunis D, et al. Neuropilin-2 acts as a modulator of Sema3A-dependent glioma cell migration. Cell Adh Migr 2009;3:383-9.
24. Epstein JA, Aghajanian H, Singh MK. Semaphorin signaling in cardiovascular development. Cell Metab 2015;21:163-73.
25. Williams G, Eickholt BJ, Maison P, Prinjha R, Walsh FS, Doherty P. A complementary peptide approach applied to the design of novel semaphorin/neuropilin antagonists. J Neurochem 2005;92:1180-90.
26. Clowes AW, Reidy MA, Clowes MM. Kinetics of cellular proliferation after arterial injury. I. Smooth muscle growth in the absence of endothelium. Lab Invest 1983;49:327-33.
27. Zou Y, Qi Y, Roztocil E, Nicholl SM, Davies MG. Patterns of kinase activation induced by injury in the murine femoral artery. J Surg Res 2007;142:332-40.
28. Pellet-Many C, Mehta V, Fields L, Mahmoud M, Lowe V, Evans I, et al. Neuropilins 1 and 2 mediate neointimal hyperplasia and re-endothelialization following arterial injury. Cardiovasc Res 2015;108:288-98.
29. Banerjee S, Sengupta K, Dhar K, Mehta S, D'Amore PA, Dhar G, et al. Breast cancer cells secreted platelet-derived growth factor-induced motility of vascular smooth muscle cells is mediated through neuropilin-1. Mol Carcinog 2006;45:871-80.
30. West DC, Rees CG, Duchesne L, Patey SJ, Terry CJ, Turnbull JE, et al. Interactions of multiple heparin binding growth factors with neuropilin-1 and potentiation of the activity of fibroblast growth factor-2. J Biol Chem 2005;280:13457-64.
31. Movassagh H, Tatari N, Shan L, Koussih L, Alsubait D, Khattabi M, et al. Human airway smooth muscle cell proliferation from asthmatics is negatively regulated by semaphorin3A. Oncotarget 2016;7:80238-51.
32. Kutschera S, Weber H, Weick A, De Smet F, Genove G, Takemoto M, et al. Differential endothelial transcriptomics identifies semaphorin 3G as a vascular class 3 semaphorin. Arterioscler Thromb Vasc Biol 2011;31:151-9.
33. Heissig B, Werb Z, Rafii S, Hattori K. Role of c-kit/Kit ligand signaling in regulating vasculogenesis. Thromb Haemost 2003;90:570-6.
34. Wang CH, Verma S, Hsieh IC, Hung A, Cheng TT, Wang SY, et al. Stem cell factor attenuates vascular smooth muscle apoptosis and increases intimal hyperplasia after vascular injury. Arterioscler Thromb Vasc Biol 2007;27:540-7.

35. Strahle U, Schmidt R. A universal program for tissue regeneration? Dev Cell 2012;23:1123-4.
36. Kiwamoto T, Ishii Y, Morishima Y, Yoh K, Maeda A, Ishizaki K, et al. Transcription factors T-bet and GATA-3 regulate development of airway remodeling. Am J Respir Crit Care Med 2006;174:142-51.
37. Lyon CA, Wadey KS, George SJ. Soluble N-cadherin: a novel inhibitor of VSMC proliferation and intimal thickening. Vascu Pharmacol 2016;78:53-62.
38. Weiser-Evans MC, Schwartz PE, Grieshaber NA, Quinn BE, Grieshaber SS, Belknap JK, et al. Novel embryonic genes are preferentially expressed by autonomously replicating rat embryonic and neointimal smooth muscle cells. Circ Res 2000;87:608-15.
39. Mellor RH, Brice G, Stanton AW, French J, Smith A, Jeffery S, et al. Mutations in FOXC2 are strongly associated with primary valve failure in veins of the lower limb. Circulation 2007;115:1912-20.
40. Munger SJ, Geng X, Srinivasan RS, Witte MH, Paul DL, Simon AM. Segregated Foxc2, NFATc1 and Connexin expression at normal developing venous valves, and Connexin-specific differences in the valve phenotypes of Cx37, Cx43, and Cx47 knockout mice. Dev Biol 2016;412:173-90.
41. Tammela T, Alitalo K. Lymphangiogenesis: molecular mechanisms and future promise. Cell 2010;140:460-76.
42. Kachlik D, Baca V, Stingl J, Sosna B, Lametschwandtner A, Minnich B, et al. Architectonic arrangement of the vasa vasorum of the human great saphenous vein. J Vasc Res 2007;44:157-66.
43. Ljungner H, Bergqvist D. Decreased fibrinolytic activity in the bottom of human vein valve pockets. Vasa 1983;12:333-6.
44. van Langevelde K, Sramek A, Rosendaal FR. The effect of aging on venous valves. Arterioscler Thromb Vasc Biol 2010;30:2075-80.
45. Labropoulos N, Summers KL, Sanchez IE, Raffetto J. Saphenous vein wall thickness in age and venous reflux-associated remodeling in adults. J Vasc Surg Venous Lymphat Disord 2017;5:216-23.
46. Henke PK, Mitsuya M, Luke CE, Elfline MA, Baldwin JF, Deatrick KB, et al. Toll-like receptor 9 signaling is critical for early experimental deep vein thrombosis resolution. Arterioscler Thromb Vasc Biol 2011;31:43-9.
47. Ellis SG, Chen MS, Jia G, Luke M, Cassano J, Lytle B. Relation of polymorphisms in five genes to long-term aortocoronary saphenous vein graft patency. Am J Cardiol 2007;99:1087-9.
48. Batchu SN, Xia J, Ko KA, Doyley MM, Abe JI, Morrell CN, et al. Axl modulates immune activation of smooth muscle cells in vein graft remodeling. Am J Physiol Heart Circ Physiol 2015;309:H1048-58.
49. Jagadeeswaran P, Cooley BC, Gross PL, Mackman N. Animal models of thrombosis from zebrafish to nonhuman primates: use in the elucidation of new pathologic pathways and the development of antithrombotic drugs. Circ Res 2016;118:1363-79.

Submitted Jan 24, 2017; accepted Mar 15, 2017.

Additional material for this article may be found online at www.jvascsurg.org.

APPENDIX (online only).

Supplementary Methods (online only)

Veins, tissue culture, and cell culture. Human saphenous vein remnants were obtained from patients undergoing coronary artery bypass or peripheral vascular bypass operations under protocols approved by the Institutional Review Boards of the University of Washington and the Benaroya Research Institute. All subjects gave informed consent. Vein sections that were marked intraoperatively with blue dye were discarded. Veins were dissected free of loose, extraneous tissue, and the veins were opened longitudinally. Endothelium was removed by gently wiping with a cotton-tipped swab. Then, segments that comprised the valve sinus or were remote from the valve sinus were selected. The valve leaflets were removed. For both types of segments, the intimal-medial layer containing smooth muscle cells (SMCs) was dissected free from the adventitia. To confirm the anatomic accuracy of the dissection of the vein wall into separate components of adventitia and intima-media, immunostaining for smooth muscle α-actin was performed on partially dissected specimens. An example is seen in Supplementary Fig 1, *A* and *B* (online only). The dissection plane goes through the outer media, leaving an intimal-medial preparation without adventitia (Supplementary Fig 1, *B*, online only).

Using a customized McIlwain tissue chopper, 2.5 mm^2 explants of the intimal-medial and adventitial layers were made. Explants (15 replicates/flask for each tissue type for each vein) were maintained in 1 mL of 20% fetal bovine serum/Dulbecco modified Eagle medium (DMEM). Migration of cells from tissue explants was assessed daily, as follows: (1) an explant was called migration positive if at least one attached, spread cell was observed outside the explant; and (2) the number of migrated cells (up to 100) was counted for each explant. The first method measures only migration, whereas the second method measures the combination of migration and postmigration proliferation.[1-3] When used, antibodies (goat anti-fibroblast growth factor 2 [FGF2][4]; chimeric anti-platelet-derived growth factor [PDGF] receptors α and β[5,6]) or peptides (SEMA3Apeptide [HAVEHGFMQTLLKVTLE], MAMpeptide [FWYHMSG SHVGTLRVKLP], or scrambled peptide control [LKHEVMFLQETVTHLAG] as described by Jiang et al[7] and made by GenScript [Piscataway, NJ]) were added with the growth medium, which was changed every 2 days.

When cells surrounding the explants became confluent (2-3 weeks), the medium was changed to Smooth Muscle Cell Growth Medium (Cell Applications, Inc, San Diego, Calif), which contains 5% fetal bovine serum and undisclosed amounts of epidermal growth factor, FGF2, insulin, and heparin (James Yu, Cell Applications, personal communication). This medium was also used for subsequent growth of passaged cells on collagen-coated plasticware (10 μg/mL bovine skin collagen in phosphate-buffered saline [PBS] overnight at 4°C).

Tissue histology and immunostaining. A different method of tissue culture was used to compare SMC proliferation and death in valve vs nonvalve tissue. After veins were cleaned of extraneous tissue and opened longitudinally, 2-cm-long specimens with contiguous valve and nonvalve areas were cut into 2-mm-wide, full-thickness (ie, with adventitia and intima-media) longitudinal specimens using the tissue chopper. These valve and nonvalve specimens were then cultured up to 4 days in 20% fetal bovine serum/DMEM. Tissue was fixed in 10% formalin at 4°C overnight and then stored in 70% ethanol until processed for embedding in paraffin. Terminal deoxynucleotidyl transferase dUTP nick end labeling staining was performed using a kit with Methyl Green counterstaining (In Situ Cell Death Detection Kit; Roche, Inc, Branchburg, NJ). For a proliferation index, immunostaining Ki67 was performed (0.5 μg/mL SP6; Abcam, Inc, Cambridge, Mass).

Cell migration, growth, and attachment. Cell migration in microchemotaxis chambers (Neuro Probe, Inc, Gaithersburg, Md) was performed as previously described.[8] For the scratch migration, assay cells were seeded at 2×10^5/well in 12-well plates. Once confluent, pressure on half of a straight-edge razor (held steady by a custom apparatus) was used to make a line in the plastic dish while cells were removed on one side with a cotton swab. The plate was turned 180 degrees, and the process was repeated so that a strip of cells 2 to 3 mm wide remained along the diameter of the dish. After washing cells with PBS and bovine basal SMC medium, cells were preincubated in bovine basal medium ± anti-PDGF receptors α and β (5 μg/mL each), anti-FGF (30 μg/mL), or immunoglobulin G. After 2 hours, 10 ng/mL of PDGF subunit BB (PDGF-BB) was added to the wells other than control wells. The cells that crossed the scratch line were counted after 48 hours.

The 3-day cell growth assay was performed by seeding 48,000 cells in 5% fetal bovine serum in bovine basal SMC medium (Cell Applications, Inc) in triplicate wells of six-well plates. The next day, triplicate wells were counted to determine plating efficiency, and the medium was changed in the remaining wells to 2% fetal bovine serum ± 10 ng/mL PDGF-BB. Preliminary experiments were performed to determine that 2% is the optimal level of serum to maintain a constant cell number. Final cell counts were performed at day 4.

For the attachment assay, 3×10^5 cells were washed once with 1 mmol/L ethylenediaminetetraacetic acid in PBS and twice with soybean trypsin inhibitor (0.5 mg/mL in PBS), then resuspended in bovine basal SMC medium containing 1 mg/mL bovine serum albumin.

Cells were then seeded into precoated (10 μg/mL bovine type I collagen in PBS, 1 hour at 37°C) 96-well plates. Uncoated wells were used as negative control. After incubation for 1 hour, the wells were washed three times, and remaining cells on the well were stained for 15 minutes with 0.2% crystal violet in 20% methanol. The dye was solubilized by adding 0.1 mol/L sodium citrate in 50% ethanol (pH 4.2) and quantified by measuring absorbance at 550 nm.

FGF2 enzyme-linked immunosorbent assay and Western blot. Cells were seeded at 2×10^5/well in six-well plates in Cell Applications SMC growth medium. The next day, the cell layer was washed and incubated for 30 minutes with serum-free bovine basal SMC medium. The medium, a heparin-releasable fraction, and the cell layer for a control group were then harvested as described previously.[9] Fresh serum-free medium was then added with 10 ng/mL PDGF-BB, and fractions were harvested at 0.5 hour, 1 hour, and 4 hours. Heparin-releasable fractions and medium were concentrated ~10-fold using Microcon-10 Ultra centrifugal filters (EMD Millipore, Billerica, Mass). Levels of FGF2 were measured using a commercial sandwich enzyme-linked immunosorbent assay for human FGF2 (DY233; R&D Systems, Minneapolis, MN).

For Western blotting, cellular proteins were extracted in HEPES extraction buffer (25 mM HEPES, pH 7.5; 5 mM ethylenediaminetetraacetic acid; 5 mM egtazic acid; 150 mM sodium chloride; 100 mM sodium pyrophosphate tetrabasic; 50 mM sodium fluoride; 1 mM benzamidine; 1% Triton X-100; 10% glycerol; 0.1% β-mercaptoethanol; 1 μg/mL pepstatin A; 5 μg/mL leupeptin; and 5 μg/mL aprotinin). The same amount of protein was size fractionated on a 10% sodium dodecyl sulfate-polyacrylamide gel, transferred to a polyvinylidene difluoride membrane (Bio-Rad, Richmond, Calif), and probed with 1 μg/mL rabbit anti-human FGF2 (sc-79; Santa Cruz Biotechnology, Santa Cruz, Calif) overnight, followed by peroxidase-conjugated anti-rabbit antibody (KPL, Gaithersburg, Md). Chemiluminescent signal development was performed using LumiGLO Reserve Chemiluminescent substrate (KPL) according to the manufacturer's protocol. Relative protein quantification was performed by scanning autoradiographs and analyzed by Image J software (National Institutes of Health, Bethesda, Md).

Immunofluorescent analysis. Subconfluent cells grown in SMC growth medium (Cell Applications, Inc) on glass coverslips were fixed in 4% paraformaldehyde for 10 minutes. The samples were permeabilized with 0.1% Triton X-100 in PBS for 2 minutes on ice. After blocking in 5% skim milk, the samples were stained with primary antibodies, including polyclonal rabbit anti-human smooth muscle myosin heavy chain (Abcam plc, Cambridge, UK) and monoclonal rabbit anti-human smooth muscle α-actin (Abcam) for 1 hour at room temperature. Corresponding secondary antibody was labeled with Alexa Fluor 555 (ThermoFisher Scientific, Waltham, Mass) for 1 hour at room temperature. The samples were mounted using the ProLong Gold Antifade Reagent with DAPI (ThermoFisher Scientific). Staining intensity was quantified using the image analysis software Image J.

RNA purification, RNA sequencing, and pathway enrichment analysis. Dissected intima-media specimens from valve and nonvalve areas (~1 cm^2/condition) were immediately placed in RNA*later* (ThermoFisher Scientific) at 4°C overnight and then frozen at −80°C until processed. Other samples was maintained in 20% fetal bovine serum/DMEM for 2 days before placement in RNA*later*. RNA was purified using TRIzol extraction coupled with Quick-RNA MiniPrep columns as instructed with DNase I treatment (Zymo Research, Irvine, Calif). The OD260/OD280 was 2.05 ± 0.02 (mean ± standard error of the mean, n = 40). Sequencing libraries were constructed from total RNA using TruSeq RNA Sample Preparation Kits v2 (Illumina, San Diego, Calif) and clustered onto a flow cell, using a cBOT amplification system with a HiSeq SR v3 Cluster Kit (Illumina). Single-read sequencing was carried out on a HiSeq2500 sequencer (Illumina), using a HiSeq SBS v3 Kit to generate 50-base reads, with a target of approximately 10 million reads per sample. FASTQs were aligned to the human reference genome to generate gene counts.

The RNA sequencing data were filtered for genes that had at least one raw count in 10% of the libraries and then normalized. The normalized data were analyzed for differentially expressed genes while blocking by donor, using voom in the limma R package.[10] The R package goseq was used to find Gene Ontology terms that were over-represented or under-represented by the differentially expressed genes in the valve and day comparisons.[11]

Statistical analysis. Repeated-measures analysis of variance (Figs 1, 2, 5, *B* and *C*, 7, and 8) was performed using SPSS (version 19; IBM Corp, Armonk, NY). Paired two-way analysis of variance (Supplementary Fig 2, *A*) and the Wilcoxon signed rank test (Figs 3, 4, 5, *A*, and 6; Supplementary Figs 2, *B-D*, and 4) were performed using Prism 6 (GraphPad Software, Inc, La Jolla, Calif). Data are presented as the mean ± standard error of the mean.

REFERENCES

1. Kenagy RD, Clowes AW. Blockade of smooth muscle cell migration and proliferation in baboon aortic explants by interleukin-1β and tumor necrosis factor-α is nitric oxide-dependent and nitric oxide-independent. J Vasc Res 2000;37:381-9.
2. Kenagy RD, Hart CE, Stetler-Stevenson WG, Clowes AW. Primate smooth muscle cell migration from aortic explants is mediated by endogenous platelet-derived growth factor and basic fibroblast growth factor acting through matrix metalloproteinases 2 and 9. Circulation 1997;96:3555-60.

3. Kenagy RD, Vergel S, Mattsson E, Bendeck M, Reidy MA, Clowes AW. The role of plasminogen, plasminogen activators, and matrix metalloproteinases in primate arterial smooth muscle cell migration. Arterioscler Thromb Vasc Biol 1996;16:1373-82.
4. Floege J, Burg M, Hugo C, Gordon KL, Van Goor H, Reidy M, et al. Endogenous fibroblast growth factor-2 mediates cytotoxicity in experimental mesangioproliferative glomerulonephritis. J Am Soc Nephrol 1998;9:792-801.
5. Englesbe MJ, Hawkins S, Hsieh PC, Davies MG, Daum G, Kenagy RD, et al. Concomitant blockade of PDGF receptors α and β induces intimal atrophy in baboon PTFE grafts. J Vasc Surg 2004;39:440-6.
6. Englesbe MJ, Davies MG, Hawkins SM, Hsieh PC, Daum G, Kenagy RD, et al. Arterial injury repair in non-human primates—the role of platelet-derived growth factor receptor-β. J Surg Res 2004;119:80-4.
7. Jiang SX, Whitehead S, Aylsworth A, Slinn J, Zurakowski B, Chan K, et al. Neuropilin 1 directly interacts with Fer kinase to mediate semaphorin 3A-induced death of cortical neurons. J Biol Chem 2010;285:9908-18.
8. Kenagy RD, Civelek M, Kikuchi S, Chen L, Grieff A, Sobel M, et al. Scavenger receptor class A member 5 (SCARA5) and suprabasin (SBSN) are hub genes of coexpression network modules associated with peripheral vein graft patency. J Vasc Surg 2016;64:202-9.e6.
9. Millette E, Rauch BH, Defawe O, Kenagy RD, Daum G, Clowes AW. Platelet-derived growth factor-BB-induced human smooth muscle cell proliferation depends on basic FGF release and FGFR-1 activation. Circ Res 2005;96:172-9.
10. Ritchie ME, Phipson B, Wu D, Hu Y, Law CW, Shi W, et al. Limma powers differential expression analyses for RNA-sequencing and microarray studies. Nucleic Acids Res 2015;43:e47.
11. Young MD, Wakefield MJ, Smyth GK, Oshlack A. Gene ontology analysis for RNA-seq: accounting for selection bias. Genome Biol 2010;11:R14.

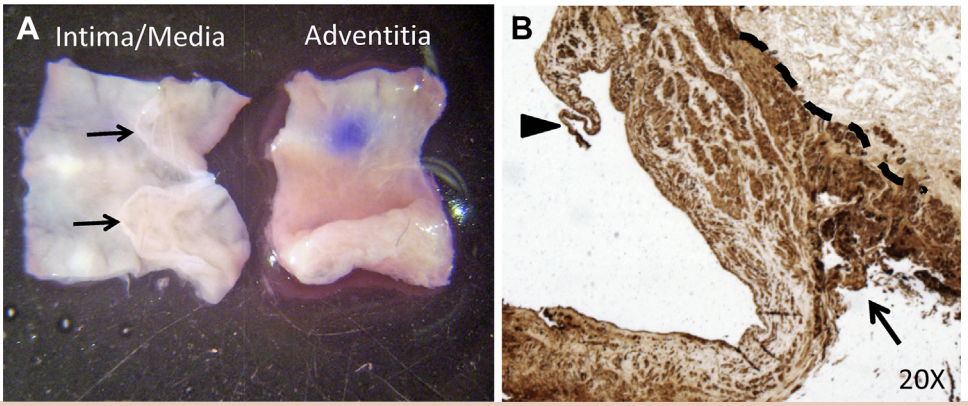

Supplementary Fig 1 (online only). Dissection of venous tissues. **A,** Representative photograph of a dissected valve sinus wall intima-media without removal of the valve leaflets (*arrows* indicate the intact valve leaflets) and the adventitia (with a *dot of blue marking dye*). **B,** Photomicrograph of a vein explant immunostained for smooth muscle α-actin. The *dashed line* marks the medial-adventitial border. The dissection plane through the outer media leaving variable amounts of media with the adventitial layer is indicated by the *arrow*. The *arrowhead* shows a valve leaflet.

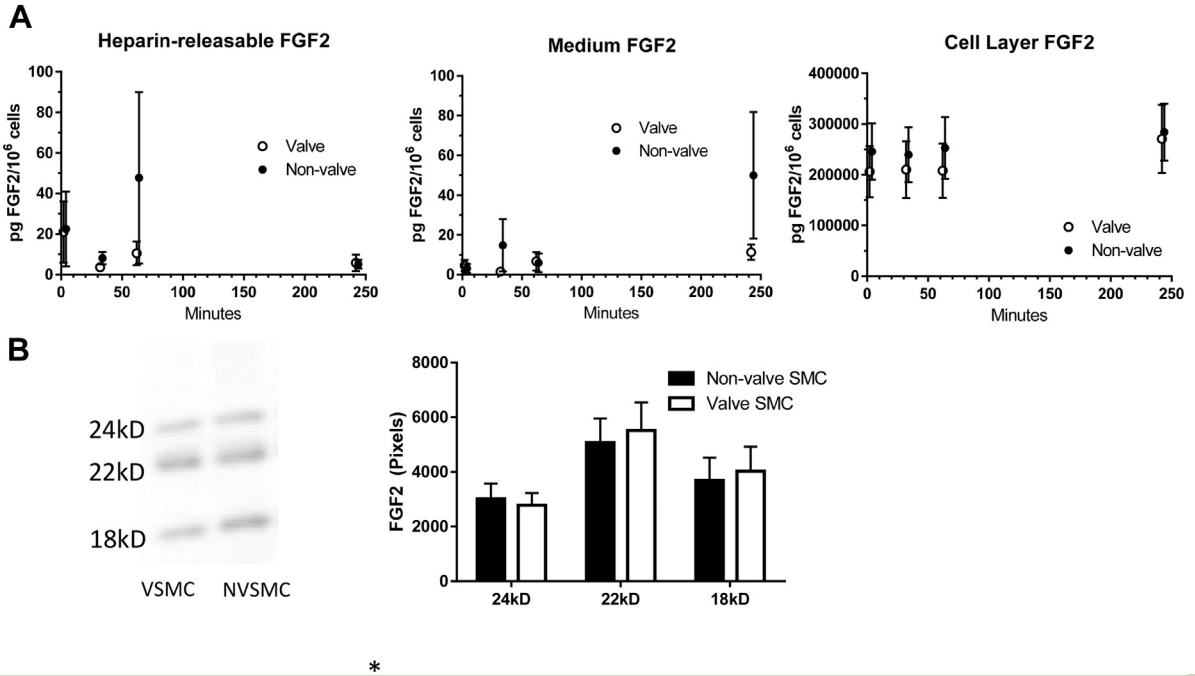

Supplementary Fig 2 (online only). Valve (*VSMC*) and nonvalve (*NVSMC*) smooth muscle cells (*SMCs*) express equivalent levels of fibroblast growth factor, but only valve SMCs migrate in response to fibroblast growth factor 2 (*FGF2*). **A,** Levels of FGF2 in the heparin-releasable fraction, medium, and cell layer (*left to right*, respectively) determined by enzyme-linked immunosorbent assay before and after treatment of valve and nonvalve SMCs with 10 ng/mL platelet-derived growth factor subunit BB (PDGF-BB) for up to 4 hours; n = 7 different pairs of valve and nonvalve SMCs for each time point. **B,** A representative Western blot of FGF2 in the total cell layer extract of valve and nonvalve SMCs is presented in the *left panel*, and quantification of the 18-kD, 22-kD, and 24-kD isoforms of FGF2 in five different pairs of valve and nonvalve SMCs is presented in the *right panel*.

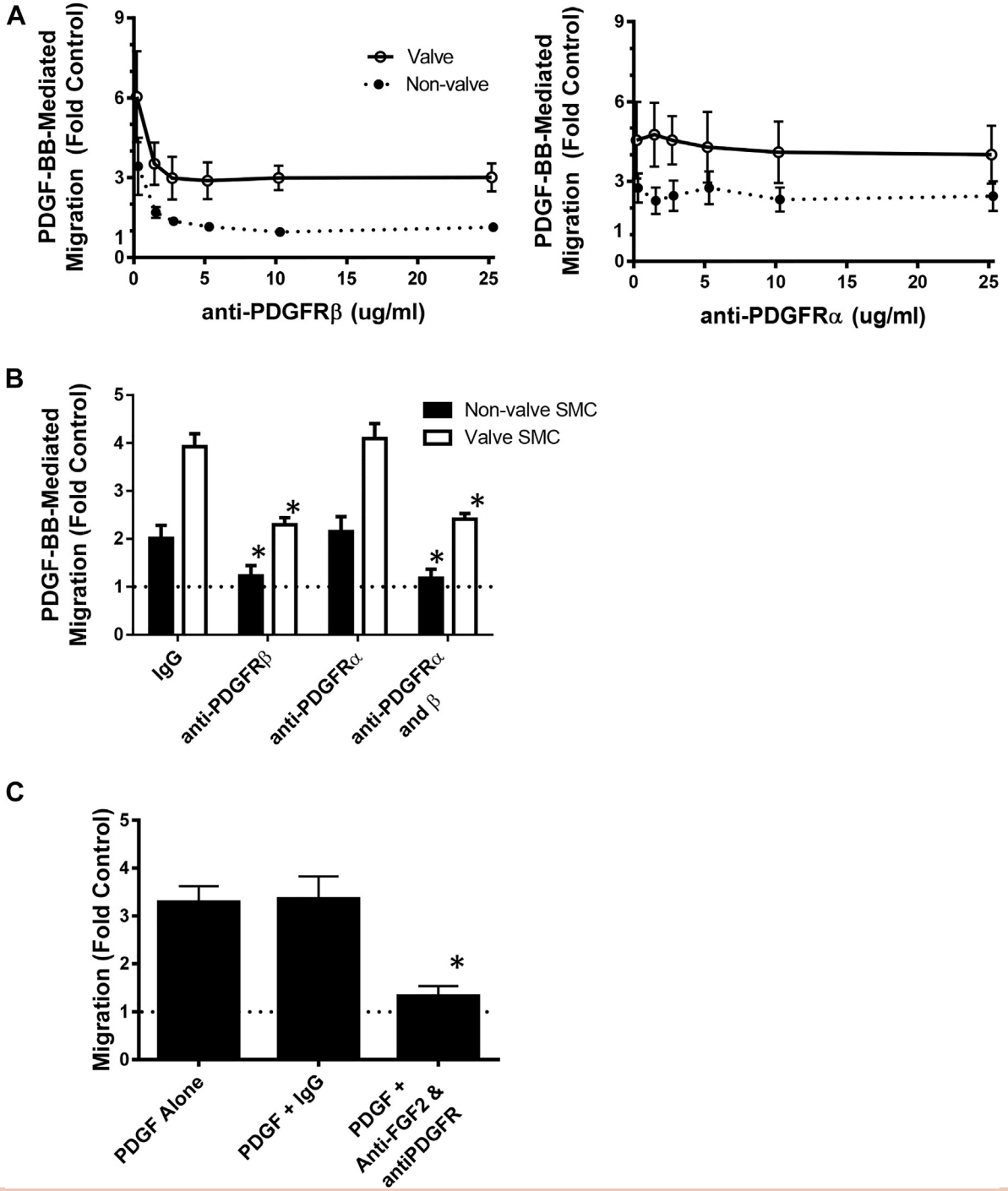

Supplementary Fig 3 (online only). Platelet-derived growth factor subunit BB (*PDGF-BB*)-mediated nonvalve smooth muscle cell (*SMC*) migration in microchemotaxis chambers is completely blocked by anti-platelet-derived growth factor receptor (*PDGFR*) β, but blockade of valve SMC migration requires a combination of anti-PDGFRβ and anti-fibroblast growth factor 2 (FGF2). **A,** Blockade by anti-PDGFRβ (*left panel*) and anti-PDGFRα (*right panel*) of valve and nonvalve SMC migration in a microchemotaxis chamber in response to 10 ng/mL PDGF-BB; n = 3 experiments performed in triplicate. **B,** Blockade of valve and nonvalve SMC migration in response to 10 ng/mL PDGF-BB by a combination of anti-PDGFRα and anti-PDGFRβ (5 μg/mL each). *$P < .05$ vs immunoglobulin G (*IgG*); n = 6 different pairs of valve and nonvalve SMCs. **C,** The effect of the combination of anti-FGF2 (30 μg/mL) and anti-PDGFRβ (10 μg/mL) on PDGF-BB-mediated valve SMC migration. *$P < .01$ vs IgG; n = 6 different pairs of valve and nonvalve SMCs.

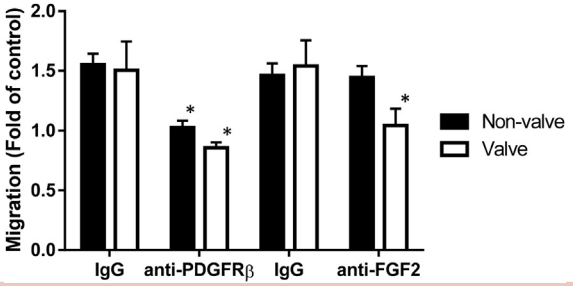

Supplementary Fig 4 (online only). Nonvalve and valve smooth muscle cell (SMC) migration in a scratch assay is completely inhibited by anti-platelet-derived growth factor receptor β (*anti-PDGFRβ*), but only valve SMC migration is inhibited by anti-fibroblast growth factor 2 (*anti-FGF2*). The effect of a blocking antibody to FGF2 (30 μg/mL) or anti-PDGFRβ (10 μg/mL) on 10 ng/mL platelet-derived growth factor subunit BB (PDGF-BB)-mediated valve vs nonvalve SMC migration in a scratch wound assay. $^*P < .05$ antibody vs immunoglobulin G (*IgG*) control; n = 3 different pairs of valve and nonvalve SMCs.

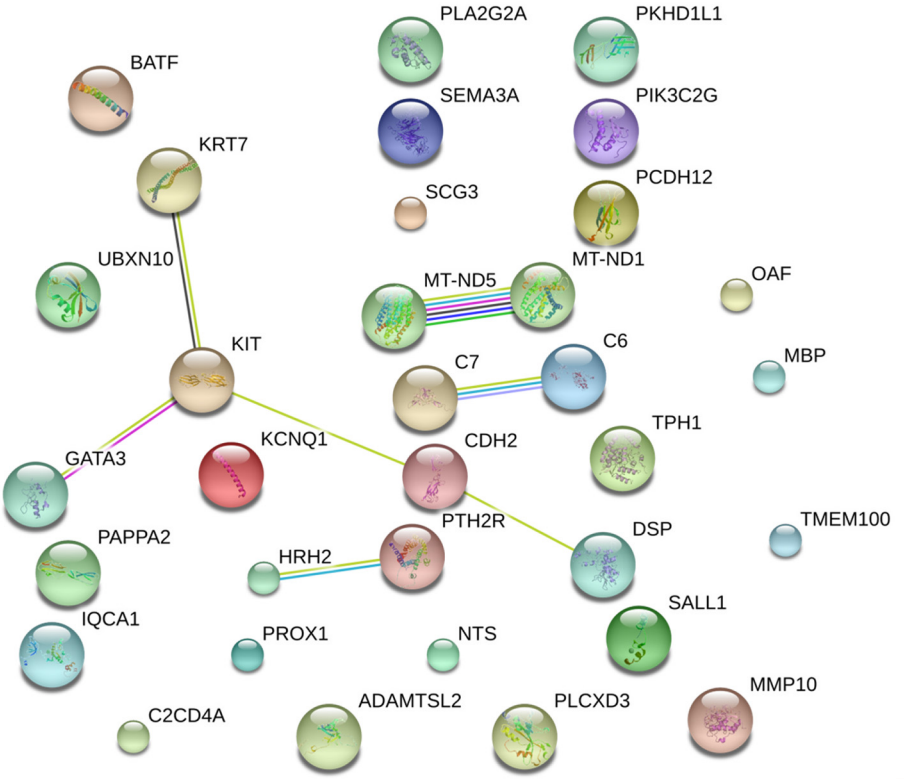

Supplementary Fig 5 (online only). STRING protein-protein interaction analysis (http://string-db.org/) of the genes differentially expressed by valve tissue demonstrates seven interactions ($P = .03$).

Supplementary Table I (online only). Genes differentially expressed in valve intimal-medial tissue

Genes differentially expressed in valve vs nonvalve tissue									
Gene	Valve vs nonvalve log fold change	*P* value	FDR	Day 2 to day 0 log fold change	*P* value	FDR	Tissue-time interaction log fold change	*P* value	FDR
BRINP3	4.52	4.8E-06	0.00817	2.624046286	.00828	0.01465	−2.004079185	.03634	0.3575
NTS	4.22	3E-06	0.0061	4.658025162	4.3E-07	1.5E-06	−4.453942666	.00014	0.10366
SCG3	3.90	7.7E-08	0.00026	1.507417093	.0394	0.06044	−2.958221051	.00224	0.19663
PLA2G2A	3.70	3.1E-10	3.2E-06	−1.757516948	.0021	0.00415	0.965102229	.20229	0.64637
PIK3C2G	3.21	1.9E-05	0.01698	−0.696433787	.43982	0.508	−0.05044735	.84471	0.97058
GATA3	3.15	4.9E-10	3.3E-06	0.203331203	.67059	0.72378	−0.549420148	.40961	0.81072
PAPPA2	3.10	1E-13	2.1E-09	−0.620396161	.11744	0.16049	−1.346469733	.0154	0.28038
PKHD1L1	2.98	4.9E-06	0.00817	−3.283193525	5E-06	1.5E-05	0.029162084	.88054	0.97807
GATA3-AS1	2.72	2.1E-08	8.7E-05	−0.434945284	.48019	0.54675	0.341218302	.62464	0.90168
BATF	2.46	2E-09	1E-05	1.855441722	7.1E-06	2.1E-05	−0.959574417	.07209	0.44842
PROX1	2.29	1.5E-06	0.00335	1.491913181	.00172	0.00345	−0.693850292	.28122	0.72309
DSP	2.28	3.8E-05	0.03185	1.032164007	.05685	0.08416	0.459274735	.54415	0.8727
UBXN10	2.27	7.2E-06	0.0086	−1.544807134	.0196	0.03206	0.052434785	.78883	0.95449
PTH2R	2.19	4.2E-07	0.00123	−0.429460991	.35819	0.4256	0.104818708	.85185	0.97257
C7	2.18	1.1E-06	0.00283	−4.205982998	1.3E-17	1.6E-16	1.129368083	.06518	0.43519
C6	2.13	6.1E-06	0.00825	−5.155309994	9.6E-15	8.5E-14	−0.213106766	.8221	0.96456
TMEM100	1.49	8.4E-06	0.00946	1.078041955	.00123	0.00253	−0.695644081	.13369	0.55026
SEMA3A	1.46	5.2E-06	0.00817	1.18229655	.00023	0.00053	−0.089866774	.83564	0.96816
ADAMTSL2	1.40	9.4E-06	0.01006	0.209970229	.50773	0.57338	−0.052817766	.90382	0.98235
HRH2	1.28	5.7E-06	0.00825	−0.138480625	.63434	0.69133	−0.740657538	.06752	0.4404
PLCXD3	1.09	7E-05	0.05266	0.295238335	.28108	0.34469	0.150597166	.69659	0.92568
OAF	0.90	1.8E-05	0.01634	1.11867518	1.2E-07	4.7E-07	−0.426933527	.14839	0.57401
MBP	−0.50	5.2E-05	0.04258	−1.267236338	1.1E-23	2.3E-22	0.422930852	.0184	0.29501
MT-ND5	−1.18	7.6E-05	0.05302	−2.55391188	2.7E-16	2.8E-15	1.017624911	.01481	0.2785
KRT7	−1.42	6.6E-05	0.0519	−0.521861216	.13268	0.17868	0.470613756	.34911	0.77691
MT-ND1	−1.43	6.9E-06	0.0086	−3.153986821	1.7E-20	2.6E-19	1.059413964	.01697	0.28954
CDH2	−1.46	1E-05	0.01026	−0.600918645	.06396	0.0934	0.550028724	.23243	0.6786
TPH1	−1.81	1.2E-05	0.01132	−3.440841862	1.9E-14	1.6E-13	1.551272578	.01158	0.2622
MMP10	−1.95	7.3E-05	0.05302	5.247289882	1.1E-25	2.9E-24	2.027061362	.00143	0.18775
Significant time-valve interaction genes									
Gene	Valve vs nonvalve log fold change	*P* value	FDR	Day 2 to day 0 log fold change	*P* value	FDR	Tissue-time interaction log fold change	*P* value	FDR
SALL1	0.56	.28543	0.8617	−0.290918464	.59772	0.65814	3.50317625	2.4E-06	0.04977
LINC01272	1.44	.00293	0.4196	5.646476196	6.1E-35	3.4E-33	−2.541327231	1.9E-05	0.05121
C2CD4A	−1.80	.01182	0.6498	1.013279778	.12064	0.16433	4.153242974	1.9E-05	0.05121
KCNQ1	−0.61	.02558	0.7615	−2.002215237	5.4E-12	3.5E-11	1.744601724	1.4E-05	0.05121
SNHG15	0.27	.12927	0.83856	1.921681054	7.9E-27	2.2E-25	−1.061855815	2E-05	0.05121
KIT	0.53	.2368	0.85388	−1.709842011	.0003	0.00068	2.914158227	8.6E-06	0.05121
IQCA1	−0.55	.2739	0.85634	−0.756648148	.13441	0.18074	3.114155967	1.6E-05	0.05121
PCDH12	−0.03	.92958	0.98953	−0.63604144	.04251	0.06469	1.894633026	2E-05	0.05121

FDR, False discovery rate.

Supplementary Table II (online only). Gene Ontology (*GO*) categories for differentially expressed genes in valve vs nonvalve

Category	Over-represented *P* value	Term	Ontology	Genes
GO:0005579	.000006	Membrane attack complex	CC	*C7, C6*
GO:0050896	.000018	Response to stimulus	BP	*PLA2G2A, GATA3, BATF, SCG3, PTH2R, C7, PROX1, NTS, BRINP3, PKHD1L1, SEMA3A, HRH2, C6, TMEM100, ADAMTSL2, PIK3C2G, DSP, PLCXD3*
GO:0002449	.000039	Lymphocyte-mediated immunity	BP	*GATA3, BATF, C7, C6*
GO:0003208	.000045	Cardiac ventricle morphogenesis	BP	*GATA3, PROX1, DSP*
GO:0002460	.000061	Adaptive immune response based on somatic recombination of immune receptors built from immunoglobulin superfamily domains	BP	*GATA3, BATF, C7, C6*
GO:0002250	.000103	Adaptive immune response	BP	*GATA3, BATF, C7, C6*
GO:0045064	.000106	T-helper 2 cell differentiation	BP	*GATA3, BATF*
GO:0002443	.000115	Leukocyte-mediated immunity	BP	*GATA3, BATF, C7, C6*
GO:0050727	.000128	Regulation of inflammatory response	BP	*PLA2G2A, GATA3, C7, C6*
GO:0071599	.000132	Otic vesicle development	BP	*GATA3, PROX1*
GO:0016064	.000141	Immunoglobulin-mediated immune response	BP	*BATF, C7, C6*
GO:0019724	.000151	B cell-mediated immunity	BP	*BATF, C7, C6*
GO:0006959	.000174	Humoral immune response	BP	*GATA3, C7, C6*
GO:0048485	.000233	Sympathetic nervous system development	BP	*GATA3, SEMA3A*
GO:0003231	.000238	Cardiac ventricle development	BP	*GATA3, PROX1, DSP*
GO:0019835	.000248	Cytolysis	BP	*C7, C6*
GO:0002526	.000284	Acute inflammatory response	BP	*GATA3, C7, C6*
GO:0003206	.000296	Cardiac chamber morphogenesis	BP	*GATA3, PROX1, DSP*
GO:0005576	.000311	Extracellular region	CC	*PAPPA2, PLA2G2A, SCG3, C7, NTS, BRINP3, PKHD1L1, SEMA3A, C6, ADAMTSL2, OAF, DSP*
GO:0071772	.000315	Response to BMP	BP	*GATA3, TMEM100*
GO:0071773	.000315	Cellular response to BMP stimulus	BP	*GATA3, TMEM100*
GO:0030855	.000330	Epithelial cell differentiation	BP	*GATA3, PROX1, HRH2, TMEM100, DSP*
GO:0006958	.000350	Complement activation, classical pathway	BP	*C7, C6*
GO:0002320	.000351	Lymphoid progenitor cell differentiation	BP	*GATA3, BATF*
GO:0051094	.000362	Positive regulation of developmental process	BP	*PLA2G2A, GATA3, PROX1, BRINP3, SEMA3A, TMEM100*
GO:0030449	.000401	Regulation of complement activation	BP	*C7, C6*
GO:2000257	.000401	Regulation of protein activation cascade	BP	*C7, C6*
GO:0032101	.000419	Regulation of response to external stimulus	BP	*PLA2G2A, GATA3, C7, SEMA3A, C6*
GO:0042092	.000464	Type 2 immune response	BP	*GATA3, BATF*
GO:1903034	.000492	Regulation of response to wounding	BP	*PLA2G2A, GATA3, C7, C6*
GO:0003205	.000566	Cardiac chamber development	BP	*GATA3, PROX1, DSP*
GO:0048863	.000679	Stem cell differentiation	BP	*PLA2G2A, BATF, PROX1, SEMA3A*
GO:0045597	.000708	Positive regulation of cell differentiation	BP	*PLA2G2A, GATA3, PROX1, BRINP3, TMEM100*
GO:0009611	.000727	Response to wounding	BP	*PLA2G2A, GATA3, SCG3, C7, C6, DSP*
GO:0010632	.000728	Regulation of epithelial cell migration	BP	*GATA3, PROX1, SEMA3A*
GO:0002455	.000760	Humoral immune response mediated by circulating immunoglobulin	BP	*C7, C6*
GO:0001709	.000787	Cell fate determination	BP	*GATA3, PROX1*

Supplementary Table II (online only). Continued.

Category	Over-represented *P* value	Term	Ontology	Genes
GO:0002920	.000811	Regulation of humoral immune response	BP	*C7, C6*
GO:0055010	.000834	Ventricular cardiac muscle tissue morphogenesis	BP	*PROX1, DSP*
GO:0006956	.000893	Complement activation	BP	*C7, C6*
GO:0048880	.000940	Sensory system development	BP	*SEMA3A*
GO:1903045	.000940	Neural crest cell migration involved in sympathetic nervous system development	BP	*SEMA3A*
GO:0009605	.000966	Response to external stimulus	BP	*PLA2G2A, GATA3, BATF, C7, PROX1, SEMA3A, C6, PIK3C2G*

BMP, Bone morphogenetic protein; *BP*, biologic process; *CC*, cellular component.

Supplementary Table III (online only). Gene Ontology (*GO*) categories for differentially expressed genes in the day-valve/nonvalve interaction

Category	Over-represented *P* value	Term	Ontology	Genes
GO:0048565	.000067	Digestive tract development	BP	*SALL1, KIT, TGFB3*
GO:0048608	.000082	Reproductive structure development	BP	*SALL1, KIT, KCNQ1, PCDH12*
GO:0055123	.000082	Digestive system development	BP	*SALL1, KIT, TGFB3*
GO:0048568	.000084	Embryonic organ development	BP	*SALL1, KIT, PCDH12, TGFB3*
GO:0061458	.000085	Reproductive system development	BP	*SALL1, KIT, KCNQ1, PCDH12*
GO:0061082	.000085	Myeloid leukocyte cytokine production	BP	*KIT, TGFB3*
GO:0022414	.000183	Reproductive process	BP	*SALL1, KIT, KCNQ1, PCDH12, TGFB3*
GO:0008406	.000208	Gonad development	BP	*SALL1, KIT, KCNQ1*
GO:0045137	.000217	Development of primary sexual characteristics	BP	*SALL1, KIT, KCNQ1*
GO:0003006	.000269	Developmental process involved in reproduction	BP	*SALL1, KIT, KCNQ1, PCDH12*
GO:0030141	.000379	Secretory granule	CC	*KIT, KCNQ1, TGFB3*
GO:0007548	.000416	Sex differentiation	BP	*SALL1, KIT, KCNQ1*
GO:0002367	.000479	Cytokine production involved in immune response	BP	*KIT, TGFB3*
GO:0060454	.000518	Positive regulation of gastric acid secretion	BP	*KCNQ1*
GO:0019955	.000924	Cytokine binding	MF	*KIT, TGFB3*

BP, Biologic process; *CC*, cellular component; *MF*, molecular function.

Supplementary Table IV (online only). Level of *SEMA3A* messenger RNA from RNA sequencing

	Day 0	Day 2
Nonvalve	22.2 ± 5.6	65.4 ± 10.2
Valve	62.2 ± 9.0	158.4 ± 38.2